

¹ **Title:** Carbon cycling in mature and regrowth forests globally: a macroecological synthesis based on the
² global Forest Carbon (ForC) database

³ **Authors:**

⁴ Kristina J. Anderson-Teixeira^{1,2*}

⁵ Valentine Herrmann¹

⁶ Becky Banbury Morgan³

⁷ Ben Bond-Lamberty⁴

⁸ Susan C. Cook-Patton⁵

⁹ Abigail E. Ferson^{1,6}

¹⁰ Helene C. Muller-Landau¹

¹¹ Maria M. H. Wang^{1,7}

¹² **Author Affiliations:**

¹³ 1. Conservation Ecology Center; Smithsonian Conservation Biology Institute; National Zoological Park,
¹⁴ Front Royal, VA 22630, USA

¹⁵ 2. Center for Tropical Forest Science-Forest Global Earth Observatory; Smithsonian Tropical Research
¹⁶ Institute; Panama, Republic of Panama

¹⁷ 3. School of Geography, University of Leeds, Leeds, UK

¹⁸ 4. Joint Global Change Research Institute, Pacific Northwest National Laboratory, College Park
¹⁹ Maryland 20740, USA

²⁰ 5. The Nature Conservancy; Arlington VA 22203, USA

²¹ 6. College of Natural Resources, University of Idaho; Moscow, Idaho 83843, USA

²² 7. Grantham Centre for Sustainable Futures and Department of Animal and Plant Sciences, University of
²³ Sheffield, Western Bank, Sheffield, South Yorkshire S10 2TN, UK

²⁴ *corresponding author: teixeirak@si.edu; +1 540 635 6546

²⁵ **NOTES TO COAUTHORS:**

- ²⁶ • “???” indicates a reference that we have entered in the .Rmd file, but not yet in the bibliography file.
²⁷ Don’t worry about those. (However, places with “REF” need references)
- ²⁸ • bold/ italic text indicates places where I know we need to go back and revisit/ fill in info

29 Summary

30 Background. Earth's climate is closely linked to forests, which strongly influence atmospheric carbon dioxide
31 (CO_2) and climate by their impact on the global carbon (C) cycle. However, efforts to incorporate forests
32 into climate models and CO_2 accounting frameworks have been constrained by a lack of accessible,
33 global-scale data on how C cycling varies across forest types and stand ages.

34 Methods/Design. Here, we draw from the Global Forest Carbon Database, ForC, to provide a macroscopic
35 overview of C cycling in the world's forests, giving special attention to stand age-related variation.

36 Specifically, we use 11923 *ForC* records from 865 geographic locations representing 34 C cycle variables to
37 characterize ensemble C budgets for four broad forest types (tropical broadleaf evergreen, temperate
38 broadleaf, temperate conifer, and taiga), including estimates for both mature and regrowth (age <100 years)
39 forests. For regrowth forests, we quantify age trends for all variables.

40 Review Results/ Synthesis. *ForC v3.0* yielded a fairly comprehensive picture of C cycling in the world's
41 major forest biomes, with broad closure of C budgets. The rate of C cycling generally increased from boreal
42 to tropical regions in both mature and regrowth forests, whereas C stocks showed less directional variation.
43 The majority of flux variables, together with most live biomass pools, increased significantly with stand age,
44 and the rate of increase again tended to increase from boreal to tropical regions.

45 Discussion. NEED TO WRITE THIS!!!

46 Key words: forest ecosystems; carbon cycle; stand age; productivity; respiration; biomass; global

47 **Background**

48 Forest ecosystems are shaping the course of climate change (IPCC1.5) through their influence on atmospheric
49 carbon dioxide (CO₂). Despite the centrality of forest C cycling in regulating atmospheric CO₂, important
50 uncertainties in climate models (???, ???, ???, Krause *et al* 2018) and CO₂ accounting frameworks (Pan *et*
51 *al* 2011) can be traced to lack of accessible, comprehensive data on how C cycling varies across forest types
52 and in relation to stand history. These require large-scale databases with global coverage, which runs
53 contrary to the nature in which forest C stocks and fluxes are measured and published. While remote sensing
54 measurements are increasingly useful for global- or regional-scale estimates of a few critical variables [e.g.,
55 aboveground biomass: (???); **REF**; gross primary productivity, *GPP*: Li and Xiao (2019); **REFS for**
56 **biomass change, net CO2 flux**], measurement of most forest C stocks and fluxes require intensive
57 on-the-ground data collection. Here, we provide a robust and comprehensive analysis of carbon cycling from
58 a stand to global level, and by biome and stand age, using the largest global compilation of forest carbon
59 data, which is available in our open source Global Carbon Forest database (ForC; Fig. 1).

60 A robust understanding of forest impacts on global C cycling is essential. Annual gross CO₂ sequestration in
61 forests (gross primary productivity, *GPP*) is estimated at >69 Gt C yr⁻¹ (???), or >7 times average annual
62 fossil fuel emissions from 2009-2018 (9.5 ± 0.5 Gt C yr⁻¹; ???). Most of this enormous C sequestration is
63 counterbalanced by CO₂ releases to the atmosphere through ecosystem respiration (*R_{eco}*) or fire, with forests
64 globally dominant as sources of both soil respiration (???) and fire emissions (REF). (check if
65 **deforestation statistic below includes natural fire, exclude here if it does.**) In recent years, the
66 remaining CO₂ sink averaged 3.2 ± 0.6 GtC yr⁻¹ from 2009-2018, offsetting 29% of anthropogenic fossil fuel
67 emissions (???). Yet, this sink is reduced by *deforestation/ forest losses to anthropogenic and natural*
68 *disturbances*. Recent net deforestation (*i.e.*, gross deforestation minus regrowth) has been a source of CO₂
69 emissions, estimated at ~1.1 Gt C yr⁻¹ from YEAR-YEAR (Pan *et al* 2011; **UPDATE**), reducing the net
70 forest sink to ~1.1-2.2 Gt C yr⁻¹ across Earth's forests (???).

71 The future of the current forest C sink is dependent both upon forest responses to climate change itself and
72 human land use decisions, which will feedback and strongly influence the course of climate change.
73 Regrowing forests in particular will play an important role (Pugh *et al* 2019), as these represent a large
74 (~#%) and growing proportion of Earth's forests (McDowell *et al* 2020). Understanding, modeling, and
75 managing forest-atmosphere CO₂ exchange is thus central to efforts to mitigate climate change [Grassi *et al*
76 (2017); Griscom *et al* (2017); **Cavaleri et al 2015**].

77 Despite the importance of forests, comprehensive global studies have historically been limited by the scattered
78 and more local nature of research studies. Primary research articles typically cover only a small numbers of
79 sites at a time. The rare exceptions that span regions or continents with rare exceptions spanning regions or
80 continents are typically coordinated through research networks such as ForestGEO (Anderson-Teixeira *et al*
81 2015, e.g., Lutz *et al* 2018) or FLUXNET [Baldocchi *et al* (2001); e.g., **FLUXNET_REF**]. The result of
82 decades of research on forest C cycling is that tens of thousands of records have been distributed across
83 literally thousands of scientific articles –often behind paywalls– along with variation in data formats, units,
84 measurement methods, *etc..* In this format, the data are effectively inaccessible for many global-scale
85 analyses, including those attempting to benchmark model performance with global data (Clark *et al* 2017,
86 Luo *et al* 2012), quantify the the role of forests in the global C cycle (*e.g.*, Pan *et al* 2011), or use
87 book-keeping methods to quantify actual or scenario-based exchanges of CO₂ between forests and the
88 atmosphere [Griscom *et al* (2017); **REFS**]. Scattered data are not conducive for advancing science nor for

89 making decisions about how to best manage our forests as a tool for constraining the climate crisis.

90 To address the need for global-scale analyses of forest C cycling, we recently developed *ForC*

91 (Anderson-Teixeira *et al* 2016, pp @anderson-teixeira_forc_2018). *ForC* contains published estimates of

92 forest ecosystem C stocks and annual fluxes (>50 variables), with the different variables capturing the unique

93 ecosystem pools (e.g., woody, foliage, and root biomass; dead wood) and flux types (e.g, gross and net

94 primary productivity; soil, root, and ecosystem respiration). These data are ground-based measurements,

95 and *ForC* contains associated data required for interpretation (e.g., stand history, measurement methods).

96 These data have been amalgamated from original peer-reviewed publications, either directly or via

97 intermediary data compilations. Since its most recent publication (Anderson-Teixeira *et al* 2018), *ForC*

98 has grown to include two additional large databases: the Global Soil Respiration Database (SRDB;

99 Bond-Lamberty and Thomson 2010) and the Global Reforestation Opportunity Assessment database

100 (GROA; Cook-Patton *et al* 2020) that also synthesized published forest C data. Following these additions,

101 *ForC* currently contains 39762 records from 10608 plots and 1532 distinct geographic areas representing all

102 forested biogeographic and climate zones. This represents an 129% increase in records from the prior

103 publication (Anderson-Teixeira *et al* 2018).

104 Here, we analyze the more extensive *ForC* data (Fig. 1) to provide a robust overview of stand-level carbon

105 cycling of the world's major forest biomes and how it varies with stand age. Our primary goal is to provide a

106 data-driven summary of our current state of knowledge on broad trends in forest C cycling. Specifically, we

107 address three broad questions:

108 1. How thoroughly can we represent C budgets for each of the world's major forest biomes (*i.e.*, tropical,

109 temperate broadleaf and deciduous, boreal) based on the current *ForC* data?

110 2. How do C cycling vary across the world's major forest biomes?

111 3. How does C cycling vary with stand age (in interaction with biome)?

112 While components of these questions have been previously addressed (Luyssaert *et al* 2007,

113 Anderson-Teixeira *et al* 2016, Cook-Patton *et al* 2020, Banbury Morgan *et al* n.d.), our analysis represents

114 by far the most comprehensive analysis of C cycling in global forests, and will serve as a foundation for

115 improved understanding of global forest C cycling and highlight where key sources of uncertainty still reside.

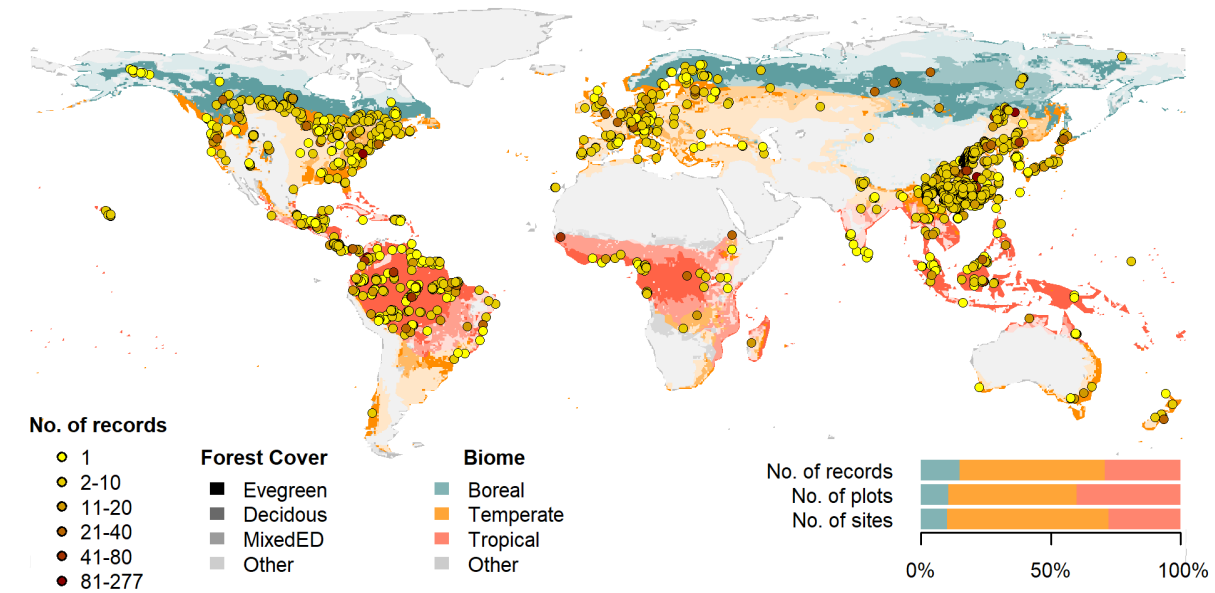


Figure 1 | Map of sites included in this analysis. Symbols are colored according to the number of records at each site. Underlying map shows coverage of evergreen, deciduous, and mixed forests (from SYNMAP; Jung et al. 2006) and biomes. Distribution of sites, plots, and records among biomes is shown in the inset.

116 Methods/ Design

117 This review synthesizes data from the *ForC* database (Fig. 1; <https://github.com/forc-db/ForC>;
 118 Anderson-Teixeira *et al* 2016, pp @anderson-teixeira_forc_2018). *ForC* amalgamates numerous
 119 intermediary data sets (*e.g.*, Luyssaert *et al* 2007, Bond-Lamberty and Thomson 2010, Cook-Patton *et al*
 120 2020) and original studies. Original publications were referenced to check values and obtain information not
 121 contained in intermediary data sets, although this process has not been completed for all records. The
 122 database was developed with goals of understanding how C cycling in forests varies across broad geographic
 123 scales and as a function of stand age. As such, there has been a focus on incorporating data from regrowth
 124 forests (*e.g.*, Anderson *et al* 2006, Martin *et al* 2013, Bonner *et al* 2013) and obtaining stand age data when
 125 possible (83% of records in v.2.0; Anderson-Teixeira *et al* 2018). Particular attention was given to developing
 126 the database for tropical forests (Anderson-Teixeira *et al* 2016), which represented roughly one-third of
 127 records in *ForC* v.2.0* (Anderson-Teixeira *et al* 2018). Since publication of *ForC* v.2.0, we added the
 128 following data to *ForC*: the Global Database of Soil Respiration Database (*SRDB* v.##, 9488 records;
 129 Bond-Lamberty and Thomson 2010), the Global Reforestation Opportunity Assessment database (*GROA*
 130 v1.0, 10116 records; Cook-Patton *et al* 2020, Anderson-Teixeira *et al* 2020). We've also added data from
 131 individual publications (detailed list at [https://github.com/forc-
 132 db/ForC/blob/master/database_management_records/ForC_data_additions_log.csv](https://github.com/forc-db/ForC/blob/master/database_management_records/ForC_data_additions_log.csv)), with a particular
 133 focus on productivity (Banbury Morgan *et al* n.d., *e.g.*, Taylor *et al* 2017), dead wood, and ForestGEO sites
 134 (*e.g.*, Lutz *et al* 2018, p @johnson_climate_2018). We note that there remains a significant amount of
 135 relevant data that is not yet included in *ForC*, particularly biomass data from national forest inventories

136 (e.g.,; **REFS**). The database version used for this analysis has been tagged as a new release on Github (**XX**)
137 and assigned a DOI through Zenodo (DOI: TBD).

138 To facilitate analyses, we created a simplified version of ForC, *ForC-simplified*
139 (https://github.com/forc-db/ForC/blob/master/ForC_simplified), which we analyzed here. In generating
140 *ForC-simplified*, all measurements originally expressed in units of dry organic matter (*OM*) were converted
141 to units of C using the IPCC default of $C = 0.47 * OM$ (IPCC 2006). Duplicate or otherwise conflicting
142 records were reconciled as described in APPENDIX S1, resulting in a total of 32499 records (81.7% size of
143 total database). Records were filtered to remove plots that had undergone significant anthropogenic
144 management or major disturbance since the most recent stand initiation event. Specifically, we removed all
145 plots flagged as managed in ForC-simplified (18.9%). This included plots with any record of managements
146 manipulating CO₂, temperature, hydrology, nutrients, or biota, as well as any plots whose site or plot name
147 contained the terms “plantation”, “planted”, “managed”, “irrigated”, or “fertilized”. Plots flagged as
148 disturbed in ForC-simplified (5.7%) included stands that had undergone any notable anthropogenic thinning
149 or partial harvest. We retained sites that were grazed or had undergone low severity natural disturbances
150 (<10% mortality) including droughts, major storms, fires, and floods. We removed all plots for which no
151 stand history information had been retrieved (7.3%). In total, this resulted in 23199 records (58.3% of the
152 records in the database) being eligible for inclusion in the analysis.

153 We selected 23 annual flux and 11 C stock variables for inclusion in the analysis. These different flux and
154 stock variables (Table 1) represent different pools (e.g., aboveground biomass, dead wood, ecosystem total)
155 and levels of combination (e.g., total aboveground net primary productivity (*ANPP*) versus the ANPP of
156 individual elements such as foliage, roots, and branches. Note that two flux variables, aboveground
157 heterotrophic (R_{het-ag}) and total (R_{het}) respiration, were included for conceptual completeness but had no
158 records in *ForC* (Table 1). Records for these variables represented 67.5% of the total records eligible for
159 inclusion. For this analysis, we combined some of ForC’s specific variables (e.g., multiple variables for net
160 primary productivity, such as measurements including or excluding fruit and flower production and herbivory)
161 into more broadly defined variables. Specifically, net ecosystem exchange (measured by eddy-covariance;
162 **FLUXNET REF**) and biometric estimates of *NEP* were combined into the single variable *NEP* (Table 1).
163 Furthermore, for *NPP*, *ANPP*, and *ANPP_{litterfall}*, *ForC* variables specifying inclusion of different
164 components were combined. Throughout ForC, for all measurements drawing from tree census data (e.g.,
165 biomass, productivity), the minimum diameter breast height (DBH) threshold for tree census was $\leq 10\text{cm}$.
166 All records were measured directly or derived from field measurements (as opposed to modeled).

167 For this analysis, we grouped forests into four broad biome types based on climate zones and dominant
168 vegetation type (tropical broadleaf, temperate broadleaf, temperate needleleaf, and boreal needleleaf) and
169 two age classifications (young and mature). Climate zones (Fig. 1) were defined based on site geographic
170 coordinates according to Köppen-Geiger zones (Rubel and Kottek 2010). We defined the tropical biome as
171 including all equatorial (A) zones, temperate biomes as including all warm temperate (C) zones and warmer
172 snow climates (Dsa, Dsb, Dwa, Dwb, Dfa, and Dfb), and the boreal biome as including the colder snow
173 climates (Dsc, Dsd, Dwc, Dwd, Dfc, and Dfd). Any forests in dry (B) and polar (E) Köppen-Geiger zones
174 were excluded from the analysis. We defined leaf type (broadleaf / needleleaf) was based on descriptions in
175 original publications (prioritized) or values extracted from a global map based on satellite observations
176 (SYNMAP; ???). For young tropical forests imported from *GROA* but not yet classified by leaf type, we
177 assumed that all were broadleaf, consistent with the rarity of naturally regenerating needleleaf forests in the

Table 1. Carbon cycle variables included in this analysis, their sample sizes, and summary of biome differences and age trends.

Variable	Description	N records			biome differences*	age trend†
		records	plots	geographic areas		
Annual fluxes						
<i>NEP</i>	net ecosystem production or net ecosystem exchange (+ indicates C sink)	329	146	88	n.s.	+; xB
<i>GPP</i>	gross primary production ($NPP + R_{auto}$ or $R_{eco} - NEE$)	303	115	84	TrB > TeB \geq TeN \geq BoN	+; xB
<i>NPP</i>	net primary production ($ANPP + BNPP$)	214	112	74	TrB > TeB \geq TeN $>$ BoN	n.s.
<i>ANPP</i>	aboveground <i>NPP</i>	343	236	131	TrB > TeB \geq TeN $>$ BoN	+; xB
<i>ANPP_{woody}</i>	woody production ($ANPP_{stem} + ANPP_{branch}$)	64	53	37	n.s.	+
<i>ANPP_{stem}</i>	woody stem production	217	190	117	TrB > TeN \geq TeB \geq BoN	n.s.
<i>ANPP_{branch}</i>	branch turnover	69	59	42	TrB > TeB \geq TeN	n.s.
<i>ANPP_{foliage}</i>	foliage production, typically estimated as annual leaf litterfall	162	132	88	TrB > TeB \geq TeN $>$ BoN	+
<i>ANPP_{litterfall}</i>	litterfall, including leaves, reproductive structures, twigs, and sometimes branches	82	70	55	n.s.	+
<i>ANPP_{repro}</i>	production of reproductive structures (flowers, fruits, seeds)	51	44	34	n.t.	n.t.
<i>ANPP_{folivory}</i>	foliar biomass consumed by folivores	20	12	11	n.t.	n.t.
<i>M_{woody}</i>	woody mortality—i.e., B_{ag} of trees that die	18	18	18	n.t.	n.t.
<i>BNPP</i>	belowground NPP ($BNPP_{coarse} + BNPP_{fine}$)	148	116	79	TrB > TeN \geq TeB \geq BoN	+
<i>BNPP_{coarse}</i>	coarse root production	77	56	36	TeN \geq TrB	n.s.
<i>BNPP_{fine}</i>	fine root production	123	99	66	n.s.	+
<i>R_{eco}</i>	ecosystem respiration ($R_{auto} + R_{het}$)	213	98	70	TrB > TeB \geq TeN	+
<i>R_{auto}</i>	autotrophic respiration ($(R_{auto-ag} + R_{root})$)	24	23	15	n.t.	n.t.
<i>R_{auto-ag}</i>	aboveground autotrophic respiration (i.e., leaves and stems)	2	2	1	n.t.	n.t.
<i>R_{root}</i>	root respiration	181	139	95	TrB \geq TeB	+
<i>R_{soil}</i>	soil respiration ($(R_{het-soil} + R_{root})$)	627	411	229	TrB > TeB $>$ TeN \geq BoN	n.s.
<i>R_{het-soil}</i>	soil heterotrophic respiration	197	156	100	TrB > TeB \geq TeN	n.s.
<i>R_{het-ag}</i>	aboveground heterotrophic respiration	0	0	0	-	-
<i>R_{het}</i>	heterotrophic respiration ($(R_{het-ag} + R_{het-soil})$)	0	0	0	-	-
Stocks						
<i>B_{tot}</i>	total live biomass ($B_{ag} + B_{root}$)	188	157	87	TrB \geq TeB $>$ BoN	+; xB
<i>B_{ag}</i>	aboveground live biomass ($B_{ag-wood} + B_{foliage}$)	4466	4072	621	TrB \geq TeN \geq TeB $>$ BoN	+; xB
<i>B_{ag-wood}</i>	woody component of aboveground biomass	115	102	64	TeN $>$ TrB \geq BoN	+; xB
<i>B_{foliage}</i>	foliage biomass	134	115	72	TeN $>$ TrB \geq BoN \geq TeB	+; xB
<i>B_{root}</i>	total root biomass ($(B_{root-coarse} + B_{root-fine})$)	2329	2298	360	n.s.	+; xB
<i>B_{root-coarse}</i>	coarse root biomass	134	120	73	TeN $>$ TeB \geq BoN	+; xB
<i>B_{root-fine}</i>	fine root biomass	226	180	109	n.s.	+; xB
<i>DW_{tot}</i>	deadwood ($DW_{standing} + DW_{down}$)	79	73	42	n.t.	+; xB
<i>DW_{standing}</i>	standing dead wood	36	35	22	n.t.	n.t.
<i>DW_{down}</i>	fallen dead wood, including coarse and sometimes fine woody debris	278	265	37	n.t.	+; xB
<i>OL</i>	organic layer / litter/ forest floor	474	413	115	n.s.	+; xB

* Tr: Tropical, TeB: Temperate Broadleaf, TeN: Temperate Needleleaf, B: Boreal, n.s.: no significant differences, n.t.: not tested

† + or -: significant positive or negative trend, xB: significant age x biome interaction, n.s.: no significant age trend, n.t.: not tested

tropics (REF). We also classified forests as “young” (< 100 years) or “mature” (≥ 100 years or classified as “mature”, “old growth”, “intact”, or “undisturbed” in original publication). Assigning stands to these

180 groupings required the exclusion of records for which *ForC* lacked geographic coordinates (0.4% of sites in
181 full database) or records of stand age (5.7% of records in full database). We also excluded records of stand
182 age = 0 year (0.8% of records in full database). In total, our analysis retained 76.1 of the focal variable
183 records for forests of known age. Numbers of records by biome and age class are given in Table S1.

184 Data were summarized to produce schematics of C cycling across the eight biome by age group combinations
185 identified above. To obtain the values reported in the C cycle schematics, we first averaged any repeated
186 measurements within a plot. Values were then averaged across geographically distinct areas, defined as plots
187 clustered within 25 km of one another (*sensu* Anderson-Teixeira *et al* 2018), weighting by area sampled if
188 available for all records. This step was taken to avoid pseudo-replication and to combine any records from
189 sites with more than one name in ForC.

190 We tested whether the C budgets described above “closed”—*i.e.*, whether they were internally consistent.
191 Specifically, we first defined relationships among variables: for example, $NEP = GPP - R_{eco}$,
192 $BNPP = BNPP_{coarse} + BNPP_{fine}$, $DW_{tot} = DW_{standing} + DW_{down}$). **(issue #44-but just delete
193 this chunk if not resolved before submission)** Henceforth, we refer to the variables on the left side of
194 the equation as “aggregate” fluxes or stocks, and those that are summed as “component” fluxes or stocks,
195 noting that the same variable can take both aggregate and component positions in different relationships.
196 We considered the C budget for a given relationship “closed” when component variables summed to within
197 one standard deviation of the aggregate variable.

198 To test for differences across mature forest biomes, we also examined how stand age impacted fluxes and
199 stocks, employing a mixed effects model [‘lmer’ function in ‘lme4’ R package version **x.xx; REF**] with biome
200 as fixed effect and plot nested within geographic.area as random effects on the intercept. When Biome had a
201 significant effect, we looked at a Tukey’s pairwise comparison to see which biomes were significantly different
202 from one another. This analysis was run for variables with records for at least seven distinct geographic areas
203 in more than one biome, excluding any biomes that failed this criteria (Table 1).

204 To test for age trends in young (<100yrs) forests, we employed a mixed effects model with biome and
205 $\log_{10}[\text{stand.age}]$ as fixed effects and plot nested within geographic.area as a random effect on the intercept.
206 This analysis was run for variables with records for at least three distinct geographic areas in more than one
207 biome, excluding any biomes that failed this criteria (Table 1). When the effect of stand age was significant
208 at $p \leq 0.05$ and when each biome had records for stands of at least 10 different ages, a biome \times stand.age
209 interaction was included in the model.

210 To facilitate the accessibility of our results and data, and to allow for rapid updates as additional data
211 become available, we have automated all database manipulation, analyses, and figure production in R
212 (**version, citation**).

213 Review Results/ Synthesis

214 Data Coverage

215 Of the 39762 records in *ForC* v3.0, 11923 met our strict criteria for inclusion in this study (Fig. 1). These
216 records were distributed across 5062 plots in 865 distinct geographic areas. Of the 23 flux and 11 stock
217 variables mapped in these diagrams, *ForC* contained sufficient mature forest data for inclusion in our
218 statistical analyses (*i.e.*, records from ≥ 7 distinct geographic areas) for 20 fluxes and 9 stocks in tropical

219 broadleaf forests, 15 fluxes and 8 stocks in temperate broadleaf forests, 14 fluxes and 7 stocks in temperate
220 conifer forests, and 8 fluxes and 7 stocks in boreal forests. For regrowth forests (<100 yrs), *ForC* contained
221 sufficient data for inclusion in our statistical analyses (*i.e.*, records from ≥ 3 distinct geographic areas) for 11
222 fluxes and 10 stocks in tropical broadleaf forests, 16 fluxes and 10 stocks in temperate broadleaf forests, 16
223 fluxes and 10 stocks in temperate conifer forests, and 14 fluxes and 9 stocks in boreal forests.

224 **C cycling in mature forests**

225 Average C cycles for mature tropical broadleaf, temperate broadleaf, temperate conifer, and boreal forests \geq
226 100 years old and with no known major natural or anthropogenic disturbance are presented in Figures 2-5
227 (and available in tabular format in the *ForC* release accompanying this publication:

228 [ForC/numbers_and_facts/ForC_variable_averages_per_Biome.csv](#)).

229 For variables with records from ≥ 7 distinct geographic areas, these ensemble C budgets were generally
230 consistent. That is, component variables summed to within one standard deviation of their respective
231 aggregate variables in all but one instance. In the temperate conifer biome, the average composite measure of
232 root biomass (B_{root}) was less than the combined average value of coarse and fine root biomass ($B_{root-coarse}$
233 and $B_{root-fine}$, respectively). This lack of closure was driven by very high estimates of $B_{root-coarse}$ from
234 high-biomass forests of the US Pacific Northwest.

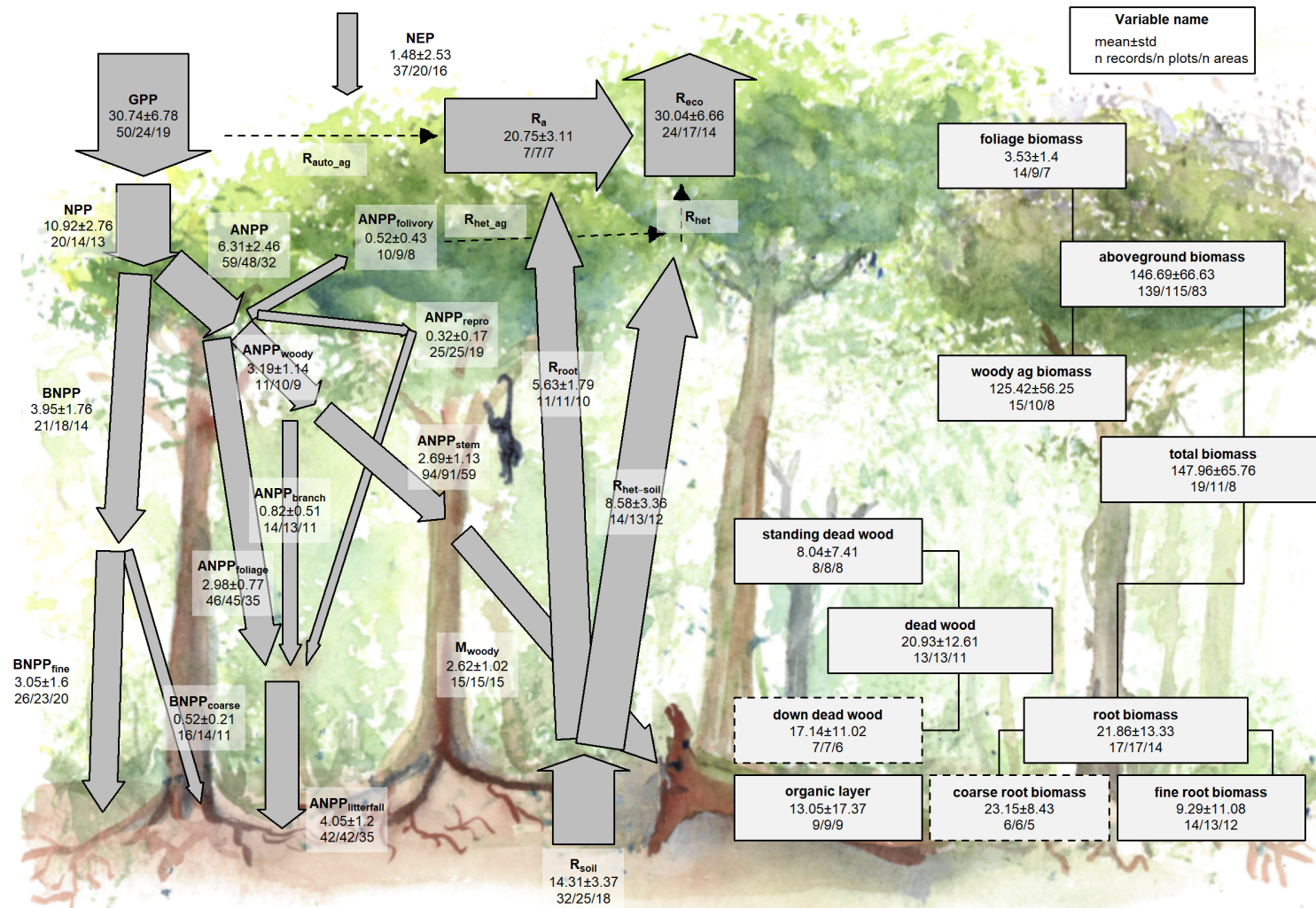


Figure 2 | C cycle diagram for mature tropical broadleaf forests. Arrows indicate fluxes ($Mg\ C\ ha^{-1}\ yr^{-1}$); boxes indicate stocks ($Mg\ C\ ha^{-1}$), with variables as defined in Table 1. Presented are mean \pm std, where geographically distinct areas are treated as the unit of replication. Dashed shape outlines indicate variables with records from <7 distinct geographic areas, and dashed arrows indicate fluxes with no data. To illustrate the magnitude of different fluxes, arrow size is proportional to the square root of corresponding flux. Asterisk after variable name indicates lack of C cycle closure.

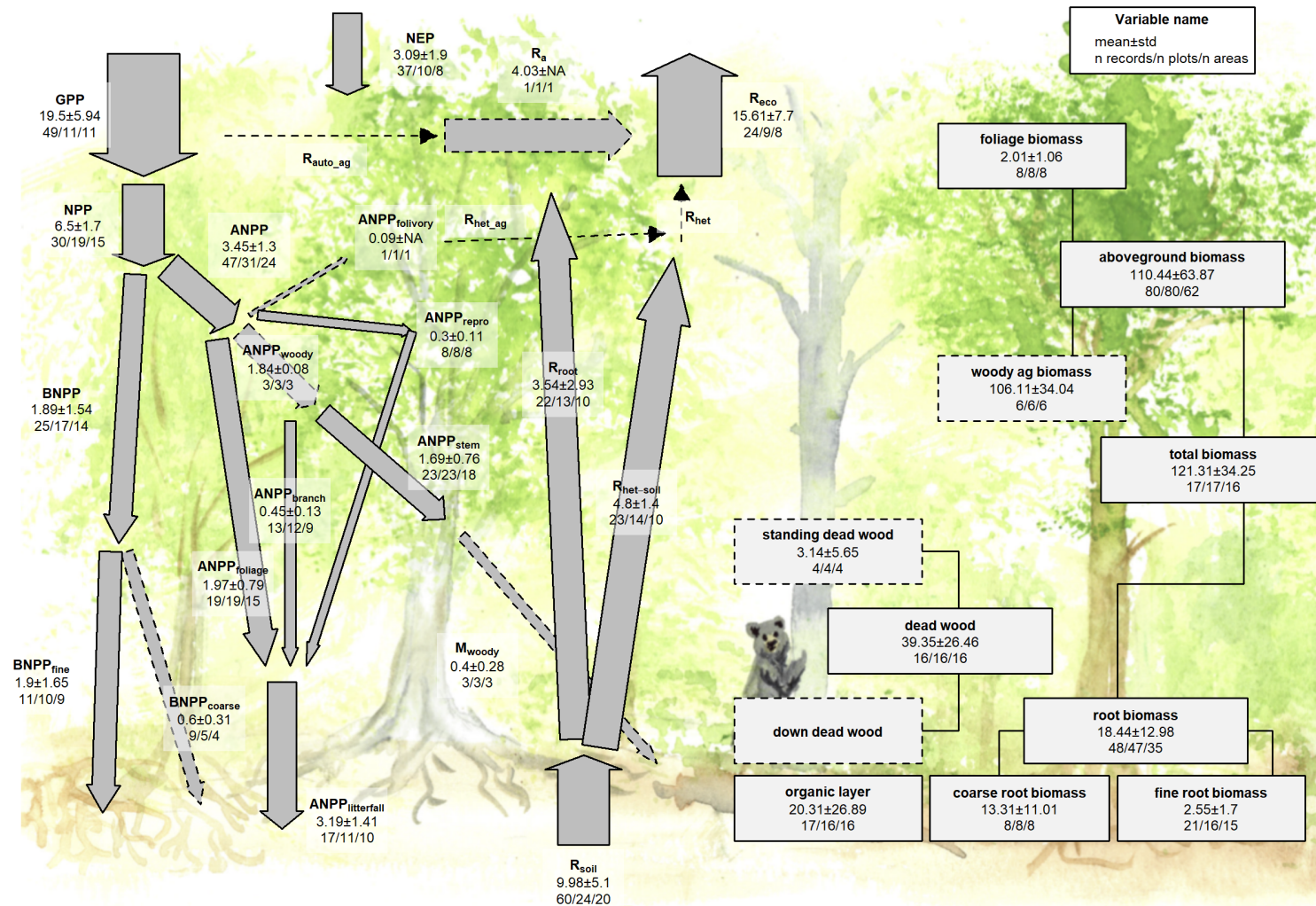


Figure 3 | C cycle diagram for mature temperate broadleaf forests. Arrows indicate fluxes ($\text{Mg C ha}^{-1} \text{ yr}^{-1}$); boxes indicate stocks (Mg C ha^{-1}), with variables as defined in Table 1. Presented are mean \pm std, where geographically distinct areas are treated as the unit of replication. Dashed shape outlines indicate variables with records from <7 distinct geographic areas, and dashed arrows indicate fluxes with no data. To illustrate the magnitude of different fluxes, arrow size is proportional to the square root of corresponding flux. Asterisk after variable name indicates lack of C cycle closure.

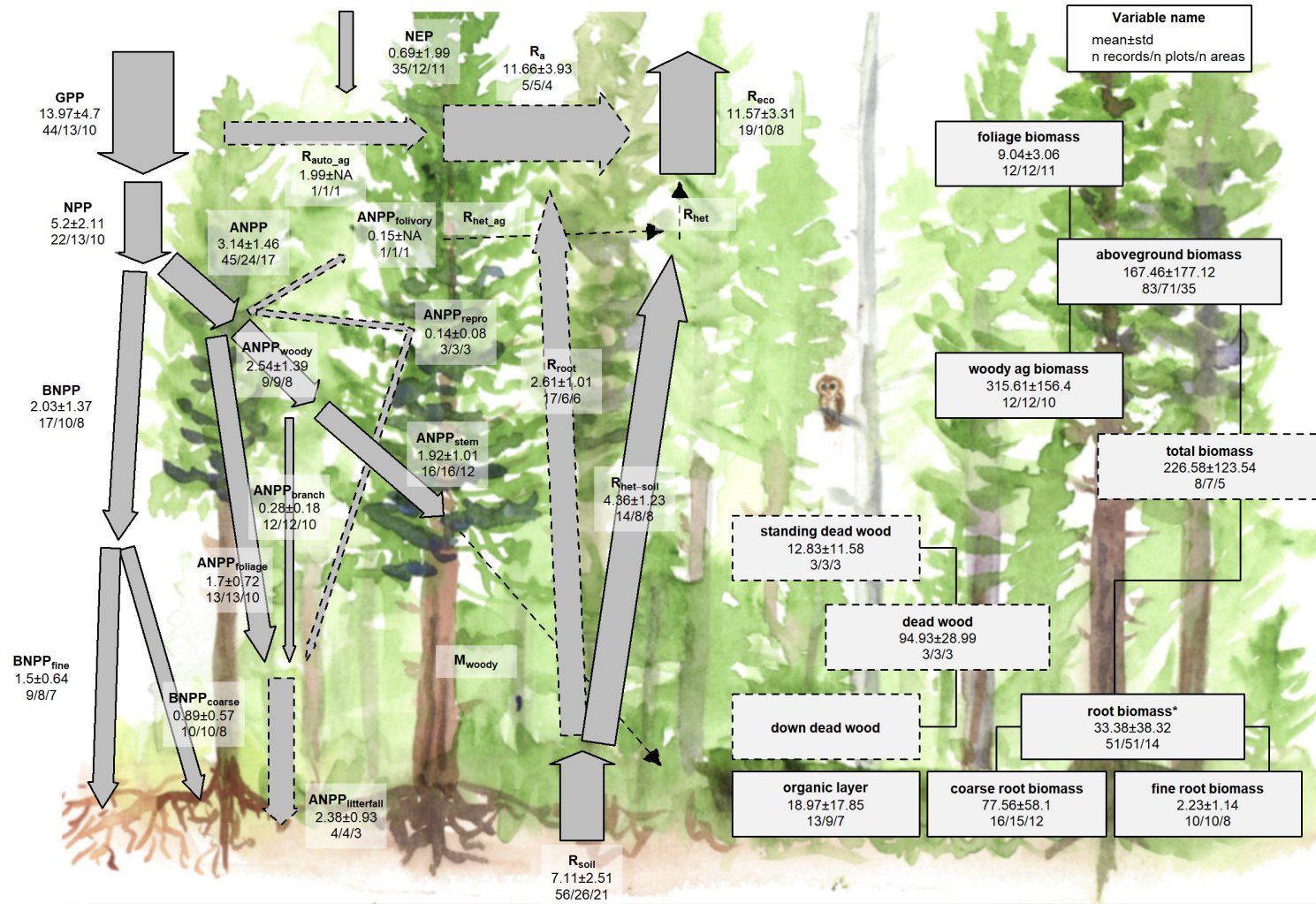


Figure 4 | C cycle diagram for mature temperate conifer forests. Arrows indicate fluxes ($\text{Mg C ha}^{-1} \text{ yr}^{-1}$); boxes indicate stocks (Mg C ha^{-1}), with variables as defined in Table 1. Presented are mean \pm std, where geographically distinct areas are treated as the unit of replication. Dashed shape outlines indicate variables with records from <7 distinct geographic areas, and dashed arrows indicate fluxes with no data. To illustrate the magnitude of different fluxes, arrow size is proportional to the square root of corresponding flux. Asterisk after variable name indicates lack of C cycle closure.

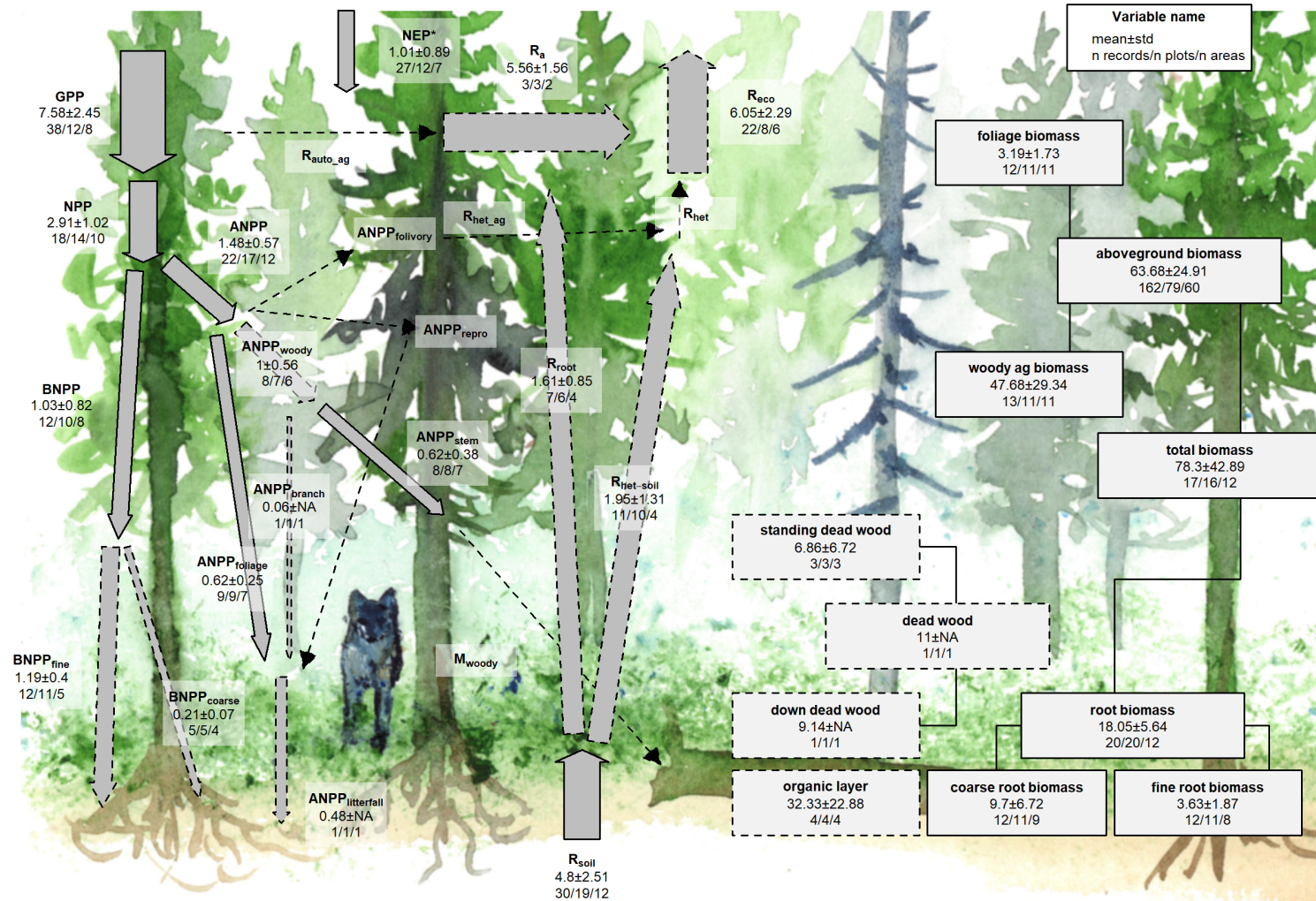


Figure 5 | C cycle diagram for mature boreal conifer forests. Arrows indicate fluxes ($\text{Mg C ha}^{-1} \text{ yr}^{-1}$); boxes indicate stocks (Mg C ha^{-1}), with variables as defined in Table 1. Presented are mean \pm std, where geographically distinct areas are treated as the unit of replication. Dashed shape outlines indicate variables with records from <7 distinct geographic areas, and dashed arrows indicate fluxes with no data. To illustrate the magnitude of different fluxes, arrow size is proportional to the square root of corresponding flux. Asterisk after variable name indicates lack of C cycle closure.

235 There were sufficient data to assess mature forest biome differences for 15 flux variables, and significant
236 differences among biomes were detected for 12 variables (Table 1). In all of these cases—including C fluxes
237 into, within, and out of the ecosystem—C fluxes were highest in tropical forests, intermediate in temperate
238 (broadleaf or conifer) forests, and lowest in boreal forests (Table 1, Figs. 6, S1-S15). Differences between
239 tropical and boreal forests were always significant, with temperate forests intermediate and significantly
240 different from one or both. Fluxes tended to be numerically greater in temperate broadleaf than conifer
241 forests, but the difference was never statistically significant. This pattern held for the following variables:
242 $GPP\$$, NPP , $ANPP$, $ANPP_{stem}$, $ANPP_{branch}$, $ANPP_{foliage}$, $BNPP$, R_{eco} , R_{root} , R_{soil} , and $R_{het-soil}$.
243 For two of the variables without significant differences among biomes ($ANPP_{litterfall}$ and $BNPP_{fine}$; Figs.
244 S8 and S11, respectively), the same general trends applied but were not statistically significant. Another
245 exception was for $BNPP_{root-coarse}$, where all records came from high-biomass forests in the US Pacific
246 Northwest, resulting in marginally higher values for the temperate conifer biome (Table 1, Fig. S10;
247 differences significant in mixed effects model but not in post-hoc pairwise comparison).

248 The most notable exception to the pattern of decreasing flux from tropical to boreal biomes was NEP , with
249 no significant differences across biomes but with the largest average in temperate broadleaf forests, followed
250 by tropical, boreal, and temperate conifer forests (Figs. 5,S1).

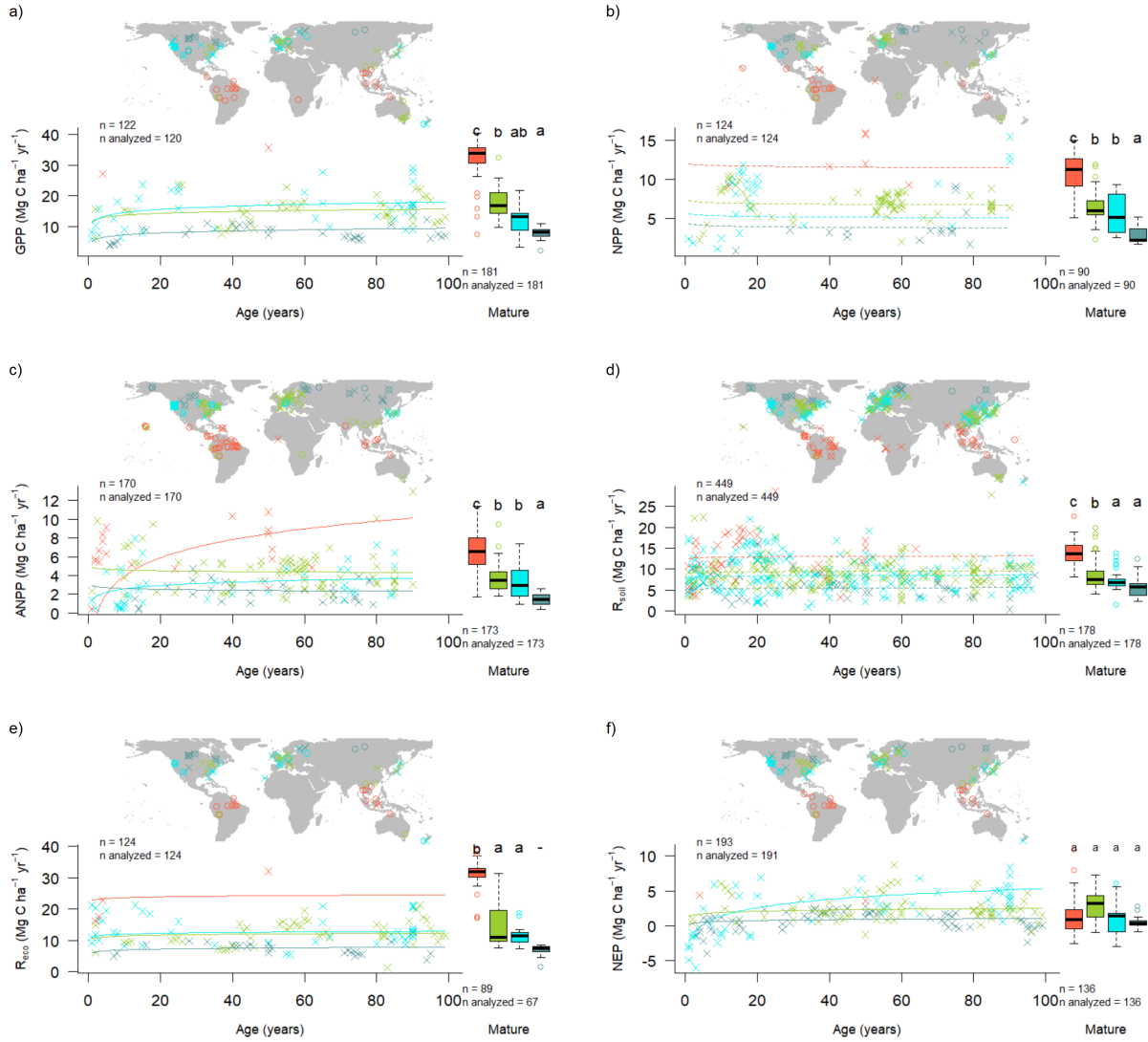


Figure 6 | Age trends and biome differences in some of the major C fluxes: (a) GPP , (b) NPP , (c) $ANPP$, (d) R_{soil} , (e) R_{eco} , and (f) NEP . Map shows data sources (x and o indicate young and mature stands, respectively). In each panel, the left scatterplot shows age trends in forests up to 100 years old, as characterized by a linear mixed effects model with fixed effects of age and biome. The fitted line indicates the effect of age on flux (solid lines: significant at $p < 0.05$, dashed lines: non-significant), and non-parallel lines indicate a significant age \times biome interaction. The boxplot illustrates distribution across mature forests, with different letters indicating significant differences between biomes. Data from biomes that did not meet the sample size criteria (see Methods) are plotted, but lack regression lines (young forests) or test of differences across biomes (mature forests). Individual figures for each flux with sufficient data are given in the Supplement (Figs. S1-S15).

251 **check this with final data (based on Table 1):** There were sufficient data to assess mature forest
 252 biome differences for **9** stock variables, and significant differences among biomes were detected for **6** variables
 253 (B_{tot} , B_{ag} , $B_{ag-wood}$, $B_{foliage}$, $B_{root-coarse}$, DW_{tot} ; Table 1). C stocks had less consistent patterns across
 254 biomes (Figs. 7, S16-S26). In **four of the six** cases (B_{tot} , $B_{ag-wood}$, $B_{root-coarse}$, DW_{tot}), temperate
 255 conifer forests had significantly higher stocks than the other biomes, and boreal forests in the lowest, with
 256 tropical and temperate broadleaf forests in between. For B_{ag} , which had by far the highest sample size,
 257 tropical forests exceeded temperate conifer forests (but not significantly). For $B_{foliage}$, temperate broadleaf
 258 forests were lowest (again, not significantly). The high values for the temperate conifer biome were driven by

259 the very high-biomass forests of the US Pacific Northwest, which are disproportionately represented in the
 260 current version of ForC. Thus, biome differences should be interpreted more as driven more by geographic
 261 distribution of sampling than by true differences.

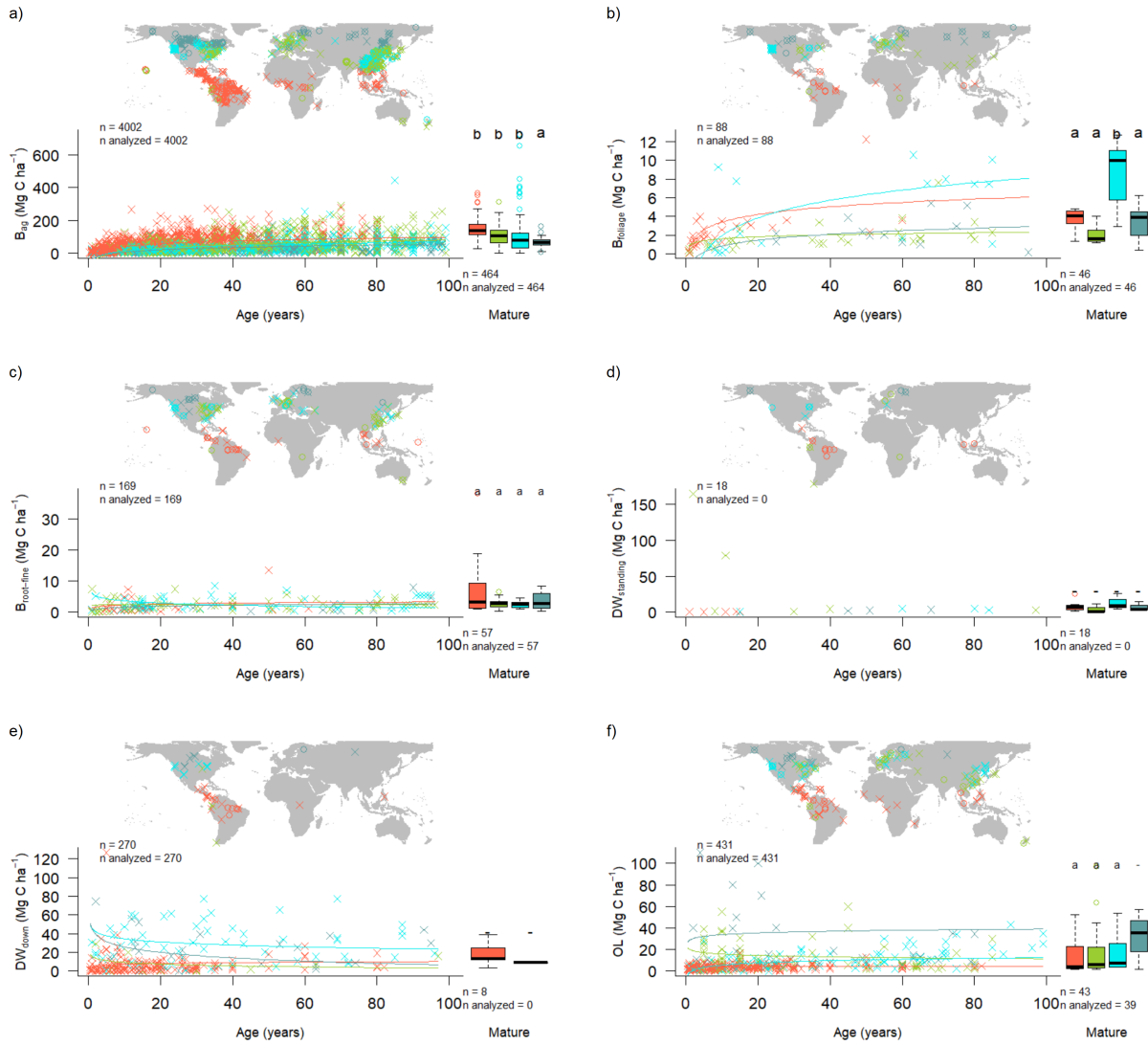


Figure 7 | Age trends and biome differences in some of the major forest C stocks: (a) aboveground biomass, (b) foliage, (c) fine roots, (d) dead wood. Map shows data sources (x and o indicate young and mature stands, respectively). In each panel, the left scatterplot shows age trends in forests up to 100 years old, as characterized by a linear mixed effects model with fixed effects of age and biome. The fitted line indicates the effect of age on flux (solid lines: significant at $p < 0.05$, dashed lines: non-significant), and non-parallel lines indicate a significant age x biome interaction. The boxplot illustrates distribution across mature forests, with different letters indicating significant differences between biomes. Data from biomes that did not meet the sample size criteria (see Methods) are plotted, but lack regression lines (young forests) or test of differences across biomes (mature forests). Individual figures for each stock with sufficient data are given in the Supplement (Figs. S16-S26).

262 C cycling in young forests

263 Average C cycles for forests < 100 years old are presented in Figures 8-11.
 264 Both C stocks and fluxes commonly increased significantly with stand age (Tables 1, S2, Figs. 6-11, S1-S26;
 265 detailed below).

266 *ForC* contained 14 flux variables with sufficient data for cross-biome analyses of age trends in regrowth
267 forests (see Methods) (Fig. 6-7 and **S#- SI figures including plots for all variables**). Of these, 9
268 increased significantly with age: *GPP*, *NPP*, *ANPP*, *ANPP_{foliage}*, *ANPP_{woody}*, *ANPP_{woody-stem}*,
269 *BNPP*, *BNPP_{root-fine}*, *R_{eco}*, and net C sequestration (*NEP*). The remaining five—*ANPP_{woody-branch}*,
270 *BNPP_{root-coarse}*, *R_{soil-het}*, and *R_{soil-het}*—displayed no significant relationship to stand age, although all
271 displayed a positive trend.

272 Differences in C fluxes across biomes typically paralleled those observed for mature forests, with C cycling
273 generally most rapid in the tropics and slowest in boreal forests.

274 The single exception was *ANPP_{stem}*, for which temperate broadleaf forests and temperate conifer forests of
275 age >~30 had slightly higher flux rates than tropical forests (*represented by a single chronosequence*).

276 Notably, the trend of tropical > temperate > boreal held for *NEP* in regrowth forests, in contrast to the
277 lack of biome differences in *NEP* for mature forests (Fig. 6).

278 There were only ## flux variables with sufficient data to test for biome x age interactions: *ANPP*,
279 *ANPP_{woody}*, *ANPP_{stem}*, *ANPP_{litterfall}*, and *BNPP* (Table S2). (**more could be added if age trends
280 become significant after outliers are resolved**) For three of these (*ANPP*, *ANPP_{litterfall}*, *BNPP*),
281 the increase in C flux with age was steepest increase in tropical forests, followed by temperate and then
282 boreal forests (Figs S#). Similarly, *ANPP_{woody}* displayed a steeper increase with age in temperate than
283 boreal forests (no tropical data for this variable). In contrast, for *ANPP_{stem}*, tropical and temperate
284 broadleaf forests had the highest flux rates at young ages, but were surpassed by temperate conifer forests
285 between ages 20 and 50 (Fig. S6).

286 (**this needs to be updated with latest data**) In terms of C stocks, 10 variables had sufficient data to
287 test for age trends. Six of these—*total biomass*, *aboveground biomass*, *aboveground woody biomass*, *foliage
288 biomass*, *root biomass*, and *coarse root biomass*—increased significantly with $\log_{10}[\text{stand.age}]$. The
289 remaining four displayed non-significant positive trends: *fine root biomass*, *total dead wood*, *standing dead
290 wood*, and *organic layer*. (*discuss rates of increase*)

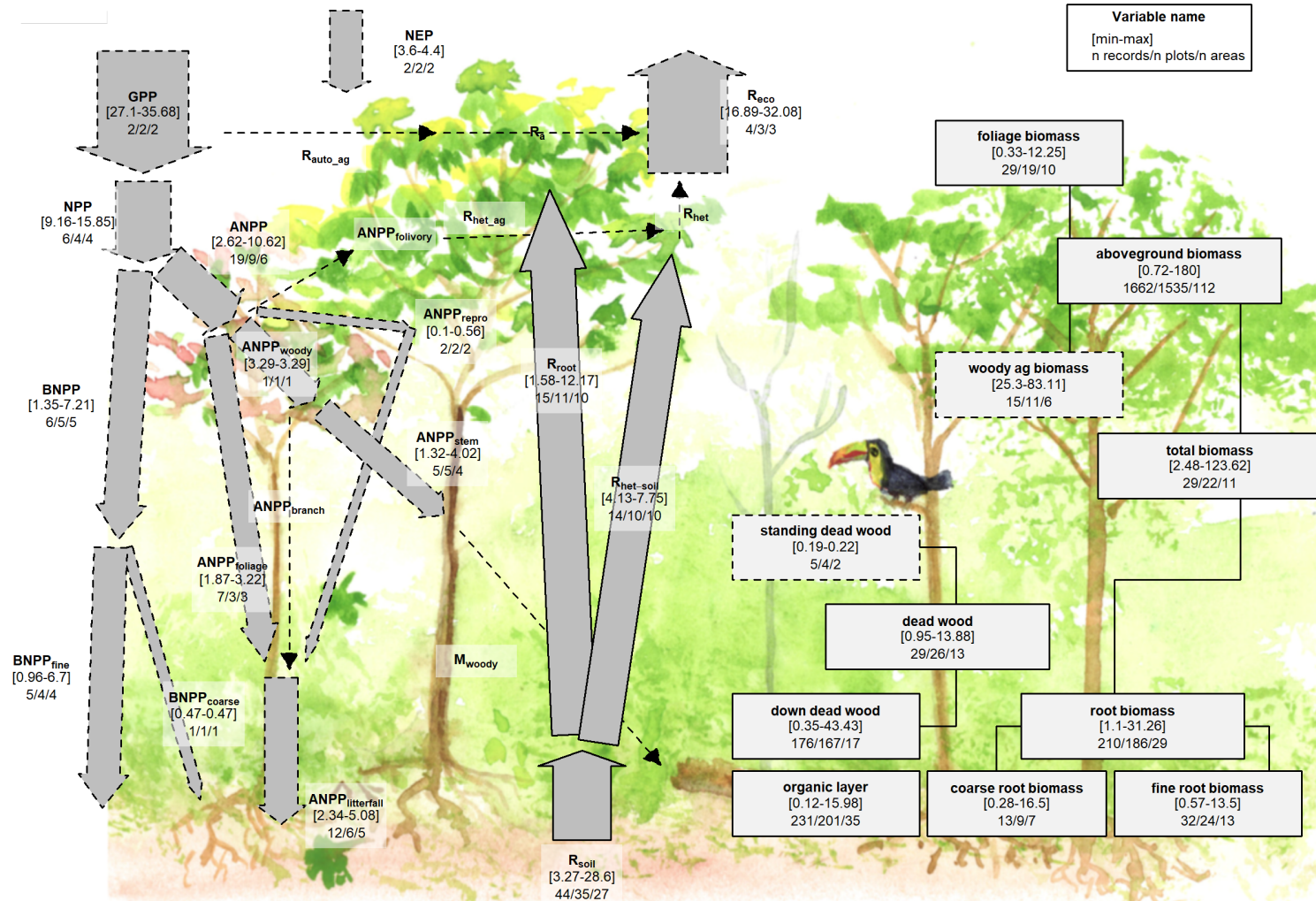


Figure 8 | C cycle diagram for young tropical broadleaf forests. Arrows indicate fluxes ($Mg\ C\ ha^{-1}\ yr^{-1}$); boxes indicate stocks ($Mg\ C\ ha^{-1}$), with variables as defined in Table 1. Presented are observed ranges, where geographically distinct areas are treated as the unit of replication. All units are $Mg\ C\ ha^{-1}\ yr^{-1}$ (fluxes) or $Mg\ C\ ha^{-1}$ (stocks). Dashed shape outlines indicate variables with records from <7 distinct geographic areas, and dashed arrows indicate fluxes with no data. To illustrate the magnitude of different fluxes, arrow size is proportional to the square root of corresponding flux.

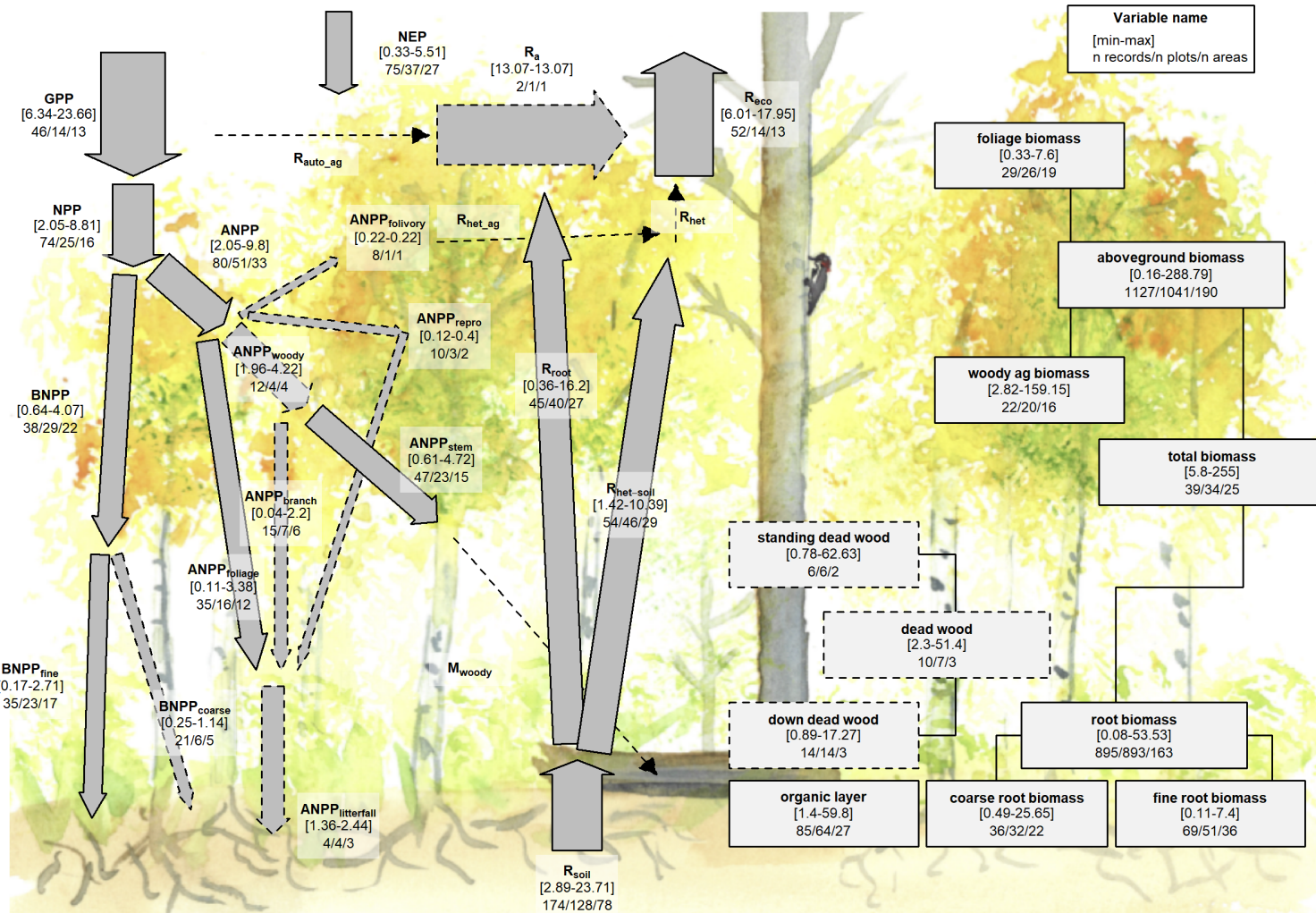


Figure 9 | C cycle diagram for young temperate broadleaf forests. Arrows indicate fluxes ($\text{Mg C ha}^{-1} \text{ yr}^{-1}$); boxes indicate stocks (Mg C ha^{-1}), with variables as defined in Table 1. Presented are observed ranges, where geographically distinct areas are treated as the unit of replication. All units are $\text{Mg C ha}^{-1} \text{ yr}^{-1}$ (fluxes) or Mg C ha^{-1} (stocks). Dashed shape outlines indicate variables with records from <7 distinct geographic areas, and dashed arrows indicate fluxes with no data. To illustrate the magnitude of different fluxes, arrow size is proportional to the square root of corresponding flux.

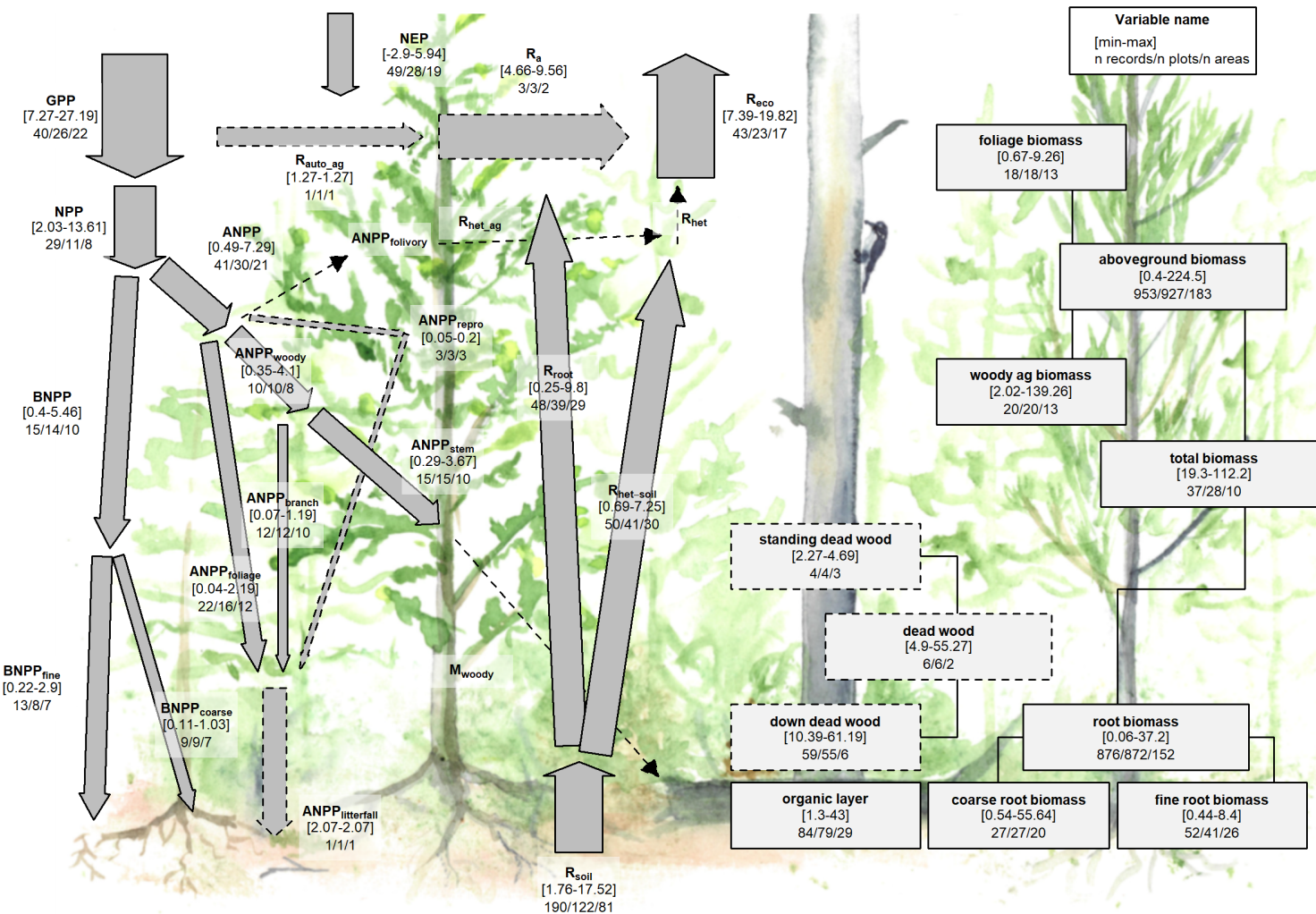


Figure 10 | C cycle diagram for young temperate conifer forests. Arrows indicate fluxes ($\text{Mg C ha}^{-1} \text{ yr}^{-1}$); boxes indicate stocks (Mg C ha^{-1}), with variables as defined in Table 1. Presented are observed ranges, where geographically distinct areas are treated as the unit of replication. All units are $\text{Mg C ha}^{-1} \text{ yr}^{-1}$ (fluxes) or Mg C ha^{-1} (stocks). Dashed shape outlines indicate variables with records from <7 distinct geographic areas, and dashed arrows indicate fluxes with no data. To illustrate the magnitude of different fluxes, arrow size is proportional to the square root of corresponding flux.

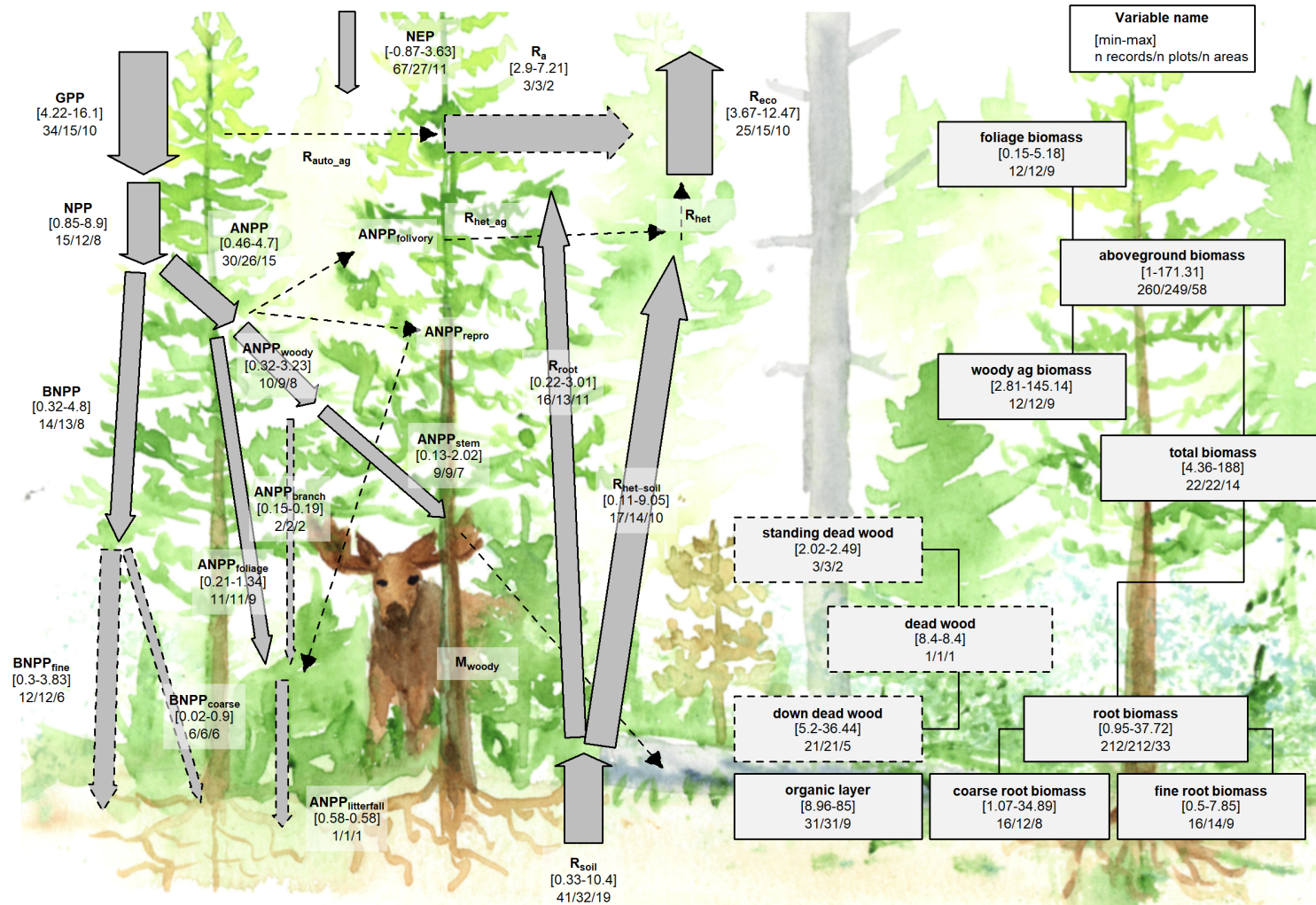


Figure 11 | C cycle diagram for young boreal conifer forests. Arrows indicate fluxes ($Mg\ C\ ha^{-1}\ yr^{-1}$); boxes indicate stocks ($Mg\ C\ ha^{-1}$), with variables as defined in Table 1. Presented are observed ranges, where geographically distinct areas are treated as the unit of replication. All units are $Mg\ C\ ha^{-1}\ yr^{-1}$ (fluxes) or $Mg\ C\ ha^{-1}$ (stocks). Dashed shape outlines indicate variables with records from <7 distinct geographic areas, and dashed arrows indicate fluxes with no data. To illustrate the magnitude of different fluxes, arrow size is proportional to the square root of corresponding flux.

291 **Discussion**

292 *ForC* v3.0 provided unprecedented coverage of most major variables, yielding an internally consistent picture
293 of C cycling in the world's major forest biomes. Carbon cycling rates generally increased from boreal to
294 tropical regions and with stand age. Specifically, the major C fluxes were highest in tropical forests,
295 intermediate in temperate (broadleaf or conifer) forests, and lowest in boreal forests – a pattern that generally
296 held for regrowth as well as mature forests (Figs. 6-7). In contrast to C fluxes, there was little directional
297 variation in mature forest C stocks across biomes (Figs. 2-5, 7). The majority of flux variables, together with
298 most live biomass pools, increased significantly with stand age (Figs. 6-11). Together, these results indicate
299 that, moving from cold to tropical climates and from young to old stands, there is a general acceleration of C
300 cycling, whereas C stocks and *NEP* of mature forests are correlated with a different set of factors.

301 **C variable coverage and budget closure**

302 The large number of C cycle variables covered by *ForC*, and the general consistency between them, provide
303 confidence that our overall reported means provide accurate and useful baselines for analysis (with the
304 caveats that they are unlikely to be accurate representations of C cycling for any particular forest, and that
305 these sample means almost certainly do not represent true biome means).

306 There are of course notable holes in the *ForC* variable coverage, as discussed by Anderson-Teixeira et
307 al. (xxxx), that limit the scope of our inferences here. Notably, *ForC* lacks coverage of fluxes to herbivores
308 and higher consumers, along with the woody mortality and dead wood stocks. Geographically, all variables
309 are poorly covered in Africa and Siberia, a common problem in the carbon-cycle community (Xu and Shang
310 2016 10.1016/j.jplph.2016.08.007, Schimel et al. 2015 10.1073/pnas.1407302112). *ForC* does not include soil
311 carbon, which is covered by other efforts (e.g. Köchy et al. 2015 10.5194/soil-1-351-2015). *ForC* is not
312 intended to replace databases that are specialized for particular parts of the C cycle analyses, e.g.,
313 aboveground biomass (REFS), land-atmosphere fluxes (Baldocchi et al. 2001
314 10.1175/1520-0477(2001)082<2415:FANTTS>2.3.CO;2), soil respiration (Jian et al. 2020
315 10.5194/essd-2020-136), or the human footprint in global forests (Magnani et al. 2007 10.1038/nature05847).

316 In this analysis, the C cycle budgets for mature forests (Figs. 2-5) generally “close”—that is, the sums of
317 component variables do not differ from the larger fluxes by more than one standard deviation. On the one
318 hand, this reflects the general fact that ecosystem-scale measurements tend to close the C budget more easily
319 and consistently than, for example, for energy balance (Stoy et al. 2013 10.1016/j.agrformet.2012.11.004). On
320 the other, however, as noted above *ForC* derives data from multiple heterogeneous sources, often with large
321 errors (standard deviations); as a result, the standard for C closure is relatively loose (cf Houghton 2020
322 10.1111/gcb.15050). Nonetheless, the lack of closure, in the few instances where it occurs, is probably more
323 reflective of differences in the representation of forest types (e.g., disproportionate representation of US
324 Pacific NW for aboveground woody biomass relative to AGB; Fig. 4) than of methodological accuracy. The
325 overall high degree of closure implies that *ForC* gives a consistent picture of C cycling within biomes. This is
326 an important and useful test, because it allows for consistency checks within the C cycle, for example
327 leveraging separate and independently-measured fluxes to constrain errors in another (Phillips et al. 2017
328 10.1007/s11104-016-3084-x, Williams et al. 2014 10.1016/j.rse.2013.10.034, Harmon et al. 2011
329 10.1029/2010JG001495), or producing internally consistent global data products (Wang et al. 2018
330 10.5194/gmd-11-3903-2018).

331 **C cycling across biomes**

332 Our analysis reveals a general deceleration of carbon cycling from the tropics to boreal regions. For mature
333 forests, this is consistent with a large body of previous work demonstrating that C fluxes generally decline
334 with latitude (or increase with temperature) on a global scale (e.g., ???, ???, Li and Xiao 2019, Banbury
335 Morgan *et al* n.d.). The consistency with which this occurs across numerous fluxes is not surprising, but has
336 never been simultaneously assessed across such a large number of variables (but see Banbury Morgan *et al*
337 n.d. for nine autotrophic fluxes). Thus, our analysis reveals that carbon cycling is most rapid in the tropics
338 and slowest in boreal regions, including C fluxes into (*GPP*), within (e.g., *NPP* and its components), and
339 out of (e.g., R_{soil} , R_{eco}) the ecosystem.

340 The notable exception to the pattern of fluxes decreasing from tropical to boreal regions is *NEP* (Fig. 6f),
341 which showed no significant differences across biomes. Unlike the other C flux variables, *NEP* does not
342 represent the rapidity with which C cycles through the ecosystem, but is the balance between C
343 sequestration (*GPP*) and respiratory losses (R_{eco}) and represents net CO₂ sequestration (or release) by the
344 ecosystem. *NEP* tends to be relatively small in mature forest stands [(???), **MORE REFS?**; discussed
345 further below], which accumulate carbon slowly relative to younger stands [(???)**; REFS**], if at all (**REFS**).
346 It is therefore unsurprising that there are no pronounced differences across biomes, suggesting that variation
347 in *NEP* of mature forests is controlled less by climate and more by other factors including moderate
348 disturbances (**REFS**) or disequilibrium of R_{soil} relative to C inputs [e.g., in peatlands where anoxic
349 conditions inhibit decomposition; **REFS**].

350 In contrast to the patterns observed for *NEP* in mature stands, *NEP* of stands between 20 and 100 years of
351 age varied across biomes, being lowest in boreal forests, intermediate in temperate broadleaf forests, and
352 highest in temperate conifer forests (with insufficient data to assess tropical forests; Figs. 6f, S1). This is
353 consistent with findings that live biomass accumulation rates (e.g., ΔB_{ag} or ΔB_{tot}) during early secondary
354 succession decrease with latitude [Anderson *et al* (2006); Cook-Patton *et al* (2020); Figs. 7a, S16-S22]. Note,
355 though, that *NEP* includes not only ΔB_{tot} , but also changes in DW_{tot} , *OL*, and soil carbon, and biome
356 differences in the accumulation rates of these variables have not been detected, in part because these variables
357 do not consistently increase with stand age [Cook-Patton *et al* (2020); Figs. 7, S23-S26; see discussion below].

358 For regrowth forests, little is known about cross-biome differences in carbon fluxes, and we are not aware of
359 any previous large-scale comparisons of C fluxes that have been limited to regrowth forests [although they're
360 commonly mixed in with mature forests; e.g., **REFS**]. Thus, this analysis was the first to examine flux
361 trends in regrowth forests across biomes. The observed tendency for young forest fluxes to decrease from
362 tropical to boreal regions paralleled patterns in mature forests (Figs. 6, S1-S15), suggesting that regrowth
363 forests follow latitudinal trends in carbon cycling similar to those of mature forests (e.g., Banbury Morgan *et*
364 *al* n.d.). Yet, *data remain sparse, and further work will be required to explore age x climate*
365 *interactions. Nevertheless, our broad-brush overview indicates that C cycling of regrowth forests is not only*
366 *higher in the tropics, parallel to fluxes in mature forests (Banbury Morgan et al n.d.), but also that it*
367 *accelerates more rapidly with stand age in the tropics, consistent with more rapid biomass accumulation.*

368 In contrast to C fluxes and biomass accumulation rates in regrowth forests, stocks showed less systematic
369 variation across biomes. For aboveground biomass, this Patterns are consistent with others studies showing
370 that variation in forest biomass across broad climatic gradients is modest and constrained more by moisture
371 than temperature (???). (???), using spaceborne lidar, showed a decline in aboveground biomass (all forests,

372 including secondary) with latitude in the N hemisphere, but values exceeding tropical forests in coastal
373 climates of both the southern and northern hemisphere. Highest biomass forests are found in temperate
374 oceanic climates (REF- , something in GEB, some global forest C map) (???). Lack of synthesis comparing
375 deadwood and organic layer across biomes, but see Cook-Patton *et al* (2020) for age trends.

376 Thus, biome differences should be interpreted more as driven more by geographic distribution of sampling
377 than by true differences.

378 Age trends in C cycling

379 (*Just some rough notes at this point*)

380 A relative dearth of data on C cycling in secondary forests, particularly in the tropics (Anderson-Teixeira et
381 al 2016), is problematic in that almost 2/3 of the world's forests were secondary as of 2010 (FAO 2010),
382 implying an under-filled need to characterize age-related trends in forest C cycling.

383 Moreover, as disturbances increase (???, McDowell *et al* 2020), understanding the carbon dynamics of
384 regrowth forests will be increasingly important.

385 It's also important to understand secondary forest C sequestration to reduce uncertainty regarding the
386 potential for carbon uptake by regrowth forests (???, Cook-Patton *et al* 2020).

387 (discuss NEP well, including) NEP increases with log(age) to 100 -> strongest C sinks are established
388 secondary forests. (But presumably this exact number is an artifact; don't over-emphasize.)

389 Our findings are largely consistent with, but built from a far larger dataset than, those of Pregitzer and
390 Euskirchen (2004 <http://dx.doi.org/10.1111/j.1365-2486.2004.00866.x>), who found that NPP and NEP to be
391 higher in intermediate-aged forests than older forests, and emphasize the importance of forest age at the
392 biome scale. Quickly-changing and age-dependent fluxes were also found in a number of previous syntheses
393 (Amiro *et al*. 2010 10.1029/2010JG001390, Magnani *et al*. 2007 10.1038/nature05847).

394 In contrast to most fluxes, *NEP* is highest at intermediate ages

395 Relevance for climate change prediction and mitigation

396 The future of forest C cycling (???) will shape trends in atmospheric CO₂ and the course of climate change.
397 For a human society seeking to understand and mitigate climate change, the data contained in *ForC* and
398 summarized here can help to meet two major challenges.

399 First, improved representation of forest C cycling in models is essential to improving predictions of the future
400 course of climate change. To ensure that models are giving the right answers for the right reasons, it is
401 important to benchmark against multiple components of the C cycle that are internally consistent with each
402 other. By making tens of thousands of records readily available in standardized format, *ForC* makes it
403 feasible for the modeling community to draw upon these data to benchmark models. Integration of *ForC*
404 with models is a goal (Fer *et al.*, in revision).

405 Second, *ForC* can serve as a pipeline through which forest science can inform forest-based climate change
406 mitigation efforts. Such efforts will be most effective when informed by the best available data, yet it is not
407 feasible for the individuals and organizations designing such efforts to sort through literature, often behind
408 paywalls, with data reported in varying units, terminology, etc. One goal for *ForC* is to serve as a pipeline

409 through which information can flow efficiently from forest researchers to decision-makers working to
410 implement forest conservation strategies at global, national, or landscape scales. This is already happening!
411 *ForC* has already contributed to updating the IPCC guidelines for carbon accounting in forests [IPCC 2019;
412 Requena Suarez *et al* (2019); Rozendaal *et al* in prep], mapping C accumulation potential from natural forest
413 regrowth globally (Cook-Patton *et al* 2020), and informing ecosystem conservation priorities (Goldstein *et al*
414 2020).

415 **ForC can complement remote sensing to provide a comprehensive picture of global forest C**
416 **cycling.** (*here, discuss what is well-covered by remote sensing, where ForC is useful for calibrating remote*
417 *sensing, and what ForC can get that remote sensing can't.*) AGB is the largest stock, and most of the
418 emphasis is on this variable. Remote sensing, with calibration based on high-quality ground-based data
419 (Schepaschenko *et al* 2019, Chave *et al* 2019), is the best approach for mapping forest carbon (REFS).
420 However, it is limited in that it is not associated with stand age and disturbance history, except in recent
421 decades when satellite data can be used to detect forest loss, gain, and some of their dominant drivers
422 (Hansen *et al* 2013, Song *et al* 2018, Curtis *et al* 2018). *ForC* is therefore valuable in defining age-based
423 trajectories in biomass, as in Cook-Patton *et al* (2020).

424 *Remote sensing measurements are increasingly useful for global- or regional-scale estimates of forest GPP*
425 *(???, Li and Xiao 2019), aboveground biomass (B_{ag}) (REFS), woody mortality (i.e., B_{ag} losses to mortality*
426 *M_{woody}) (Clark *et al* 2004, Leitold *et al* 2018), and to some extent net ecosystem exchange (NEP) (REFS).*
427 Other variables, in particular respiration fluxes, cannot be remotely sensed ((??)), and efforts such as the

428 Global Carbon Project (**le quere REF**) and NASA CMS (**citation:**
429 https://carbon.nasa.gov/pdfs/CMS_Phase-1_Report_Final_optimized.pdf but maybe
430 better to cite open literature, one of the papers listed at
431 <https://cmsflux.jpl.nasa.gov/get-data/publication-data-sets>) typically compute them as residuals
432 only. (**Ben, it would be particularly helpful if you could flesh this out some more.**)

433 In terms of C stocks, there is a paucity of data on dead wood and organic layer (Pan *et al.* ?). These can be
434 significant. (**Note that we've given a lot of emphasis to dead wood (work by Abby), and as a**
435 **result this work really advances knowledge of dead wood. We'll want to highlight that here.**)
436 (*give some stats/ cite figures*).

437 **Move to data availability statement, or methods?:** We recommend that use of *ForC* data go to the
438 original database, as opposed to using “off-the-shelf” values from this publication. This is because (1) *ForC*
439 is constantly being updated, (2) analyses should be designed to match the application, (3) age equations
440 presented here all fit a single functional form that is not necessarily the best possible for all the variables.

441 As climate change accelerates, understanding and managing the carbon dynamics of forests will be critical to
442 forecasting, mitigation, and adaptation. The C data in *ForC*, as summarized here, will be valuable to these
443 efforts.

444 Acknowledgements

445 Thanks to all researchers whose data are included in *ForC* and this analysis, to Jennifer McGarvey and Ian
446 McGregor for help with the database, and to Norbert Kunert for helpful discussion. Funding sources
447 included a Smithsonian Scholarly Studies grant to KAT and HML and a Smithsonian Working Land and
448 Seascapes grant to KAT.

449 **Data availability statement**

450 Materials required to fully reproduce these analyses, including data, R scripts, and image files, are archived
451 in Zenodo (DOI: TBD]. Data, scripts, and results presented here are also available through the open-access
452 *ForC* GitHub repository (<https://github.com/forc-db/ForC>), where many will be updated as the database
453 develops.

454 **ORCID iD**

455 Kristina J. Anderson-Teixeira: <https://orcid.org/0000-0001-8461-9713>

456 **References**

- 457 Anderson K J, Allen A P, Gillooly J F and Brown J H 2006 Temperature-dependence of biomass
458 accumulation rates during secondary succession *Ecology Letters* **9** 673–82 Online:
459 <http://www.blackwell-synergy.com/doi/abs/10.1111/j.1461-0248.2006.00914.x>
- 460 Anderson-Teixeira K, Herrmann V, CookPatton, Ferson A and Lister K 2020 Forc-db/GROA: Release with
461 Cook-Patton et al. 2020, Nature. Online: <https://zenodo.org/record/3983644>
- 462 Anderson-Teixeira K J, Davies S J, Bennett A C, Gonzalez-Akre E B, Muller-Landau H C, Joseph Wright S,
463 Abu Salim K, Almeyda Zambrano A M, Alonso A, Baltzer J L, Basset Y, Bourg N A, Broadbent E N,
464 Brockelman W Y, Bunyavejchewin S, Burslem D F R P, Butt N, Cao M, Cardenas D, Chuyong G B, Clay K,
465 Cordell S, Dattaraja H S, Deng X, Detto M, Du X, Duque A, Erikson D L, Ewango C E N, Fischer G A,
466 Fletcher C, Foster R B, Giardina C P, Gilbert G S, Gunatilleke N, Gunatilleke S, Hao Z, Hargrove W W,
467 Hart T B, Hau B C H, He F, Hoffman F M, Howe R W, Hubbell S P, Inman-Narahari F M, Jansen P A,
468 Jiang M, Johnson D J, Kanzaki M, Kassim A R, Kenfack D, Kibet S, Kinnaird M F, Korte L, Kral K,
469 Kumar J, Larson A J, Li Y, Li X, Liu S, Lum S K Y, Lutz J A, Ma K, Maddalena D M, Makana J-R, Malhi
470 Y, Marthews T, Mat Serudin R, McMahon S M, McShea W J, Memiaghe H R, Mi X, Mizuno T, Morecroft
471 M, Myers J A, Novotny V, Oliveira A A de, Ong P S, Orwig D A, Ostertag R, Ouden J den, Parker G G,
472 Phillips R P, Sack L, Sainge M N, Sang W, Sri-ngernyuang K, Sukumar R, Sun I-F, Sungpalee W, Suresh H
473 S, Tan S, Thomas S C, Thomas D W, Thompson J, Turner B L, Uriarte M, Valencia R, et al 2015
474 CTFS-ForestGEO: A worldwide network monitoring forests in an era of global change *Global Change Biology*
475 **21** 528–49 Online: <http://onlinelibrary.wiley.com/doi/10.1111/gcb.12712/abstract>
- 476 Anderson-Teixeira K J, Wang M M H, McGarvey J C, Herrmann V, Tepley A J, Bond-Lamberty B and
477 LeBauer D S 2018 ForC: A global database of forest carbon stocks and fluxes *Ecology* **99** 1507–7 Online:
478 <http://doi.wiley.com/10.1002/ecy.2229>
- 479 Anderson-Teixeira K J, Wang M M H, McGarvey J C and LeBauer D S 2016 Carbon dynamics of mature
480 and regrowth tropical forests derived from a pantropical database (TropForC-db) *Global Change Biology* **22**
481 1690–709 Online: <http://onlinelibrary.wiley.com/doi/10.1111/gcb.13226/abstract>
- 482 Baldocchi D, Falge E, Gu L, Olson R, Hollinger D, Running S, Anthoni P, Bernhofer C, Davis K, Evans R,
483 Fuentes J, Goldstein A, Katul G, Law B, Lee X, Malhi Y, Meyers T, Munger W, Oechel W, Paw K T,
484 Pilegaard K, Schmid H P, Valentini R, Verma S, Vesala T, Wilson K and Wofsy S 2001 FLUXNET: A New
485 Tool to Study the Temporal and Spatial Variability of Ecosystem-Scale Carbon Dioxide, Water Vapor, and

- 486 Energy Flux Densities *Bulletin of the American Meteorological Society* **82** 2415–34 Online:
 487 [http://journals.ametsoc.org/doi/abs/10.1175/1520-0477\(2001\)082%3C2415:FANTTS%3E2.3.CO;2](http://journals.ametsoc.org/doi/abs/10.1175/1520-0477(2001)082%3C2415:FANTTS%3E2.3.CO;2)
- 488 Banbury Morgan B, Herrmann V, Kunert N, Bond-Lamberty B, Muller-Landau H C and Anderson-Teixeira
 489 K J Global patterns of forest autotrophic carbon fluxes *Global Change Biology*
- 490 Bond-Lamberty B and Thomson A 2010 A global database of soil respiration data *Biogeosciences* **7** 1915–26
 491 Online: <http://www.biogeosciences.net/7/1915/2010/>
- 492 Chave J, Davies S J, Phillips O L, Lewis S L, Sist P, Schepaschenko D, Armston J, Baker T R, Coomes D,
 493 Disney M, Duncanson L, Héault B, Labrière N, Meyer V, Réjou-Méchain M, Scipal K and Saatchi S 2019
 494 Ground Data are Essential for Biomass Remote Sensing Missions *Surveys in Geophysics* **40** 863–80 Online:
 495 <https://doi.org/10.1007/s10712-019-09528-w>
- 496 Clark D B, Castro C S, Alvarado L D A and Read J M 2004 Quantifying mortality of tropical rain forest
 497 trees using high-spatial-resolution satellite data *Ecology Letters* **7** 52–9 Online:
 498 <https://onlinelibrary.wiley.com/doi/abs/10.1046/j.1461-0248.2003.00547.x>
- 499 Cook-Patton S C, Leavitt S M, Gibbs D, Harris N L, Lister K, Anderson-Teixeira K J, Briggs R D, Chazdon
 500 R L, Crowther T W, Ellis P W, Griscom H P, Herrmann V, Holl K D, Houghton R A, Larrosa C, Lomax G,
 501 Lucas R, Madsen P, Malhi Y, Paquette A, Parker J D, Paul K, Routh D, Roxburgh S, Saatchi S, Hoogen J
 502 van den, Walker W S, Wheeler C E, Wood S A, Xu L and Griscom B W 2020 Mapping carbon accumulation
 503 potential from global natural forest regrowth *Nature* **585** 545–50 Online:
 504 <http://www.nature.com/articles/s41586-020-2686-x>
- 505 Curtis P G, Slay C M, Harris N L, Tyukavina A and Hansen M C 2018 Classifying drivers of global forest
 506 loss *Science* **361** 1108–11 Online: <http://science.sciencemag.org/content/361/6407/1108>
- 507 Goldstein A, Turner W R, Spawn S A, Anderson-Teixeira K J, Cook-Patton S, Fargione J, Gibbs H K,
 508 Griscom B, Hewson J H, Howard J F, Ledezma J C, Page S, Koh L P, Rockström J, Sanderman J and Hole
 509 D G 2020 Protecting irrecoverable carbon in Earth's ecosystems *Nature Climate Change* 1–9 Online:
 510 <http://www.nature.com/articles/s41558-020-0738-8>
- 511 Grassi G, House J, Dentener F, Federici S, Elzen M den and Penman J 2017 The key role of forests in
 512 meeting climate targets requires science for credible mitigation *Nature Climate Change* **7** 220–6 Online:
 513 <https://www.nature.com/articles/nclimate3227>
- 514 Griscom B W, Adams J, Ellis P W, Houghton R A, Lomax G, Miteva D A, Schlesinger W H, Shoch D,
 515 Siikamäki J V, Smith P, Woodbury P, Zganjar C, Blackman A, Campari J, Conant R T, Delgado C, Elias P,
 516 Gopalakrishna T, Hamsik M R, Herrero M, Kiesecker J, Landis E, Laestadius L, Leavitt S M, Minnemeyer S,
 517 Polasky S, Potapov P, Putz F E, Sanderman J, Silvius M, Wollenberg E and Fargione J 2017 Natural climate
 518 solutions *Proceedings of the National Academy of Sciences* **114** 11645–50 Online:
 519 <http://www.pnas.org/lookup/doi/10.1073/pnas.1710465114>
- 520 Hansen M C, Potapov P V, Moore R, Hancher M, Turubanova S A, Tyukavina A, Thau D, Stehman S V,
 521 Goetz S J, Loveland T R, Kommareddy A, Egorov A, Chini L, Justice C O and Townshend J R G 2013
 522 High-Resolution Global Maps of 21st-Century Forest Cover Change *Science* **342** 850–3 Online:
 523 <http://www.sciencemag.org/cgi/doi/10.1126/science.1244693>
- 524 Johnson D J, Needham J, Xu C, Massoud E C, Davies S J, Anderson-Teixeira K J, Bunyavejchewin S,

- 525 Chambers J Q, Chang-Yang C-H, Chiang J-M, Chuyong G B, Condit R, Cordell S, Fletcher C, Giardina C P,
 526 Giambelluca T W, Gunatilleke N, Gunatilleke S, Hsieh C-F, Hubbell S, Inman-Narahari F, Kassim A R,
 527 Katabuchi M, Kenfack D, Litton C M, Lum S, Mohamad M, Nasardin M, Ong P S, Ostertag R, Sack L,
 528 Swenson N G, Sun I F, Tan S, Thomas D W, Thompson J, Umaña M N, Uriarte M, Valencia R, Yap S,
 529 Zimmerman J, McDowell N G and McMahon S M 2018 Climate sensitive size-dependent survival in tropical
 530 trees *Nature Ecology & Evolution* **2** 1436–42 Online: <http://www.nature.com/articles/s41559-018-0626-z>
 531 Krause A, Pugh T A M, Bayer A D, Li W, Leung F, Bondeau A, Doelman J C, Humpenöder F, Anthoni P,
 532 Bodirsky B L, Ciais P, Müller C, Murray-Tortarolo G, Olin S, Popp A, Sitch S, Stehfest E and Arneth A
 533 2018 Large uncertainty in carbon uptake potential of land-based climate-change mitigation efforts *Global
 534 Change Biology* **24** 3025–38 Online: <https://onlinelibrary.wiley.com/doi/abs/10.1111/gcb.14144>
 535 Leitold V, Morton D C, Longo M, dos-Santos M N, Keller M and Scaranello M 2018 El Niño drought
 536 increased canopy turnover in Amazon forests *New Phytologist* **219** 959–71 Online:
 537 <http://doi.wiley.com/10.1111/nph.15110>
 538 Li X and Xiao J 2019 Mapping Photosynthesis Solely from Solar-Induced Chlorophyll Fluorescence: A
 539 Global, Fine-Resolution Dataset of Gross Primary Production Derived from OCO-2 *Remote Sensing* **11** 2563
 540 Online: <https://www.mdpi.com/2072-4292/11/21/2563>
 541 Lutz J A, Furniss T J, Johnson D J, Davies S J, Allen D, Alonso A, Anderson-Teixeira K J, Andrade A,
 542 Baltzer J, Becker K M L, Blomdahl E M, Bourg N A, Bunyavejchewin S, Burslem D F R P, Cansler C A,
 543 Cao K, Cao M, Cárdenas D, Chang L-W, Chao K-J, Chao W-C, Chiang J-M, Chu C, Chuyong G B, Clay K,
 544 Condit R, Cordell S, Dattaraja H S, Duque A, Ewango C E N, Fischer G A, Fletcher C, Freund J A,
 545 Giardina C, Germain S J, Gilbert G S, Hao Z, Hart T, Hau B C H, He F, Hector A, Howe R W, Hsieh C-F,
 546 Hu Y-H, Hubbell S P, Inman-Narahari F M, Itoh A, Janík D, Kassim A R, Kenfack D, Korte L, Král K,
 547 Larson A J, Li Y, Lin Y, Liu S, Lum S, Ma K, Makana J-R, Malhi Y, McMahon S M, McShea W J,
 548 Memiaghe H R, Mi X, Morecroft M, Musili P M, Myers J A, Novotny V, Oliveira A de, Ong P, Orwig D A,
 549 Ostertag R, Parker G G, Patankar R, Phillips R P, Reynolds G, Sack L, Song G-Z M, Su S-H, Sukumar R,
 550 Sun I-F, Suresh H S, Swanson M E, Tan S, Thomas D W, Thompson J, Uriarte M, Valencia R, Vicentini A,
 551 Vrška T, Wang X, Weiblen G D, Wolf A, Wu S-H, Xu H, Yamakura T, Yap S and Zimmerman J K 2018
 552 Global importance of large-diameter trees *Global Ecology and Biogeography* **27** 849–64 Online:
 553 <https://onlinelibrary.wiley.com/doi/abs/10.1111/geb.12747>
 554 Luyssaert S, Inglima I, Jung M, Richardson A D, Reichstein M, Papale D, Piao S L, Schulze E-D, Wingate L,
 555 Matteucci G, Aragao L, Aubinet M, Beer C, Bernhofer C, Black K G, Bonal D, Bonnefond J-M, Chambers J,
 556 Ciais P, Cook B, Davis K J, Dolman A J, Gielen B, Goulden M, Grace J, Granier A, Grelle A, Griffis T,
 557 Grünwald T, Guidolotti G, Hanson P J, Harding R, Hollinger D Y, Hutyra L R, Kolari P, Kruijt B, Kutsch
 558 W, Lagergren F, Laurila T, Law B E, Maire G L, Lindroth A, Loustau D, Malhi Y, Mateus J, Migliavacca M,
 559 Misson L, Montagnani L, Moncrieff J, Moors E, Munger J W, Nikinmaa E, Ollinger S V, Pita G, Rebmann
 560 C, Roupsard O, Saigusa N, Sanz M J, Seufert G, Sierra C, Smith M-L, Tang J, Valentini R, Vesala T and
 561 Janssens I A 2007 CO₂ balance of boreal, temperate, and tropical forests derived from a global database
 562 *Global Change Biology* **13** 2509–37 Online:
 563 <http://onlinelibrary.wiley.com/doi/abs/10.1111/j.1365-2486.2007.01439.x>
 564 McDowell N G, Allen C D, Anderson-Teixeira K, Aukema B H, Bond-Lamberty B, Chini L, Clark J S,
 565 Dietze M, Grossiord C, Hanbury-Brown A, Hurtt G C, Jackson R B, Johnson D J, Kueppers L, Lichstein J

- 566 W, Ogle K, Poulter B, Pugh T A M, Seidl R, Turner M G, Uriarte M, Walker A P and Xu C 2020 Pervasive
 567 shifts in forest dynamics in a changing world *Science* **368** Online:
 568 <https://science.sciencemag.org/content/368/6494/eaaz9463>
- 569 Pan Y, Birdsey R A, Fang J, Houghton R, Kauppi P E, Kurz W A, Phillips O L, Shvidenko A, Lewis S L,
 570 Canadell J G, Ciais P, Jackson R B, Pacala S, McGuire A D, Piao S, Rautiainen A, Sitch S and Hayes D
 571 2011 A Large and Persistent Carbon Sink in the World's Forests *Science* **333** 988–93 Online:
 572 <http://www.sciencemag.org/content/early/2011/07/27/science.1201609.abstract>
- 573 Pugh T A M, Lindeskog M, Smith B, Poulter B, Arneth A, Haverd V and Calle L 2019 Role of forest
 574 regrowth in global carbon sink dynamics *Proceedings of the National Academy of Sciences* **116** 4382–7
 575 Online: <http://www.pnas.org/lookup/doi/10.1073/pnas.1810512116>
- 576 Requena Suarez D, Rozendaal D M A, Sy V D, Phillips O L, Alvarez-Dávila E, Anderson-Teixeira K,
 577 Araujo-Murakami A, Arroyo L, Baker T R, Bongers F, Brienen R J W, Carter S, Cook-Patton S C,
 578 Feldpausch T R, Griscom B W, Harris N, Héroult B, Coronado E N H, Leavitt S M, Lewis S L, Marimon B
 579 S, Mendoza A M, N'dja J K, N'Guessan A E, Poorter L, Qie L, Rutishauser E, Sist P, Sonké B, Sullivan M J
 580 P, Vilanova E, Wang M M H, Martius C and Herold M 2019 Estimating aboveground net biomass change for
 581 tropical and subtropical forests: Refinement of IPCC default rates using forest plot data *Global Change
 582 Biology* **25** 3609–24 Online: <http://onlinelibrary.wiley.com/doi/abs/10.1111/gcb.14767>
- 583 Schepaschenko D, Chave J, Phillips O L, Lewis S L, Davies S J, Réjou-Méchain M, Sist P, Scipal K, Perger
 584 C, Herault B, Labrière N, Hofhansl F, Affum-Baffoe K, Aleinikov A, Alonso A, Amani C, Araujo-Murakami
 585 A, Armston J, Arroyo L, Ascarrunz N, Azevedo C, Baker T, Bałazy R, Bedeau C, Berry N, Bilous A M,
 586 Bilous S Y, Bissiengou P, Blanc L, Bobkova K S, Braslavskaya T, Brienen R, Burslem D F R P, Condit R,
 587 Cuni-Sánchez A, Danilina D, Torres D del C, Derroire G, Descroix L, Sotta E D, d'Oliveira M V N, Dresel C,
 588 Erwin T, Evdokimenko M D, Falck J, Feldpausch T R, Foli E G, Foster R, Fritz S, Garcia-Abril A D,
 589 Gornov A, Gornova M, Gothard-Basséché E, Gourlet-Fleury S, Guedes M, Hamer K C, Susanty F H, Higuchi
 590 N, Coronado E N H, Hubau W, Hubbell S, Ilstedt U, Ivanov V V, Kanashiro M, Karlsson A, Karminov V N,
 591 Killeen T, Koffi J-C K, Konovalova M, Kraxner F, Krejza J, Krisnawati H, Krivobokov L V, Kuznetsov M A,
 592 Lakyda I, Lakyda P I, Licona J C, Lucas R M, Lukina N, Lussetti D, Malhi Y, Manzanera J A, Marimon B,
 593 Junior B H M, Martinez R V, Martynenko O V, Matsala M, Matyashuk R K, Mazzei L, Memiaghe H,
 594 Mendoza C, Mendoza A M, Morozuk O V, Mukhortova L, Musa S, Nazimova D I, Okuda T, Oliveira L C,
 595 et al 2019 The Forest Observation System, building a global reference dataset for remote sensing of forest
 596 biomass *Scientific Data* **6** 1–11 Online: <http://www.nature.com/articles/s41597-019-0196-1>
- 597 Song X-P, Hansen M C, Stehman S V, Potapov P V, Tyukavina A, Vermote E F and Townshend J R 2018
 598 Global land change from 1982 to 2016 *Nature* **560** 639–43 Online:
 599 <http://www.nature.com/articles/s41586-018-0411-9/>
- 600 Taylor P G, Cleveland C C, Wieder W R, Sullivan B W, Doughty C E, Dobrowski S Z and Townsend A R
 601 2017 Temperature and rainfall interact to control carbon cycling in tropical forests ed L Liu *Ecology Letters*
 602 **20** 779–88 Online: <http://doi.wiley.com/10.1111/ele.12765>